TECHNOLOGY DEPT.

First Copy

The 'ENGLISH ELECTRIC' Journal

PUBLIC LIBRARY
APR 19 1957
DETROIT

VOLUME FIFTEEN · NUMBER ONE

MARCH 1957

With the compliments of

ENGLISH ELECTRIC EXPORT & TRADING CO. LTD.

23 BEAVER STREET, NEW YORK 4, N.Y. *Telephone: WHITEHALL 4-8969*

Agent for West Coast Territories:
JAMES I. METCALF & CO. INC.
ROOM 701, UNITED PACIFIC BUILDING, SEATTLE 4, WASHINGTON,

THE
ENGLISH ELECTRIC
JOURNAL

VOLUME FIFTEEN • NUMBER ONE • MARCH 1957

A

THE ENGLISH ELECTRIC JOURNAL

VOLUME FIFTEEN NUMBER ONE MARCH 1957

CONTENTS

Page 5 : SALIME HYDRO-ELECTRIC POWER STATION IN SPAIN, *by H. S. Pound-Corner, M.A., A.M.I.E.E.*

18 : A LINCOLN AIRCRAFT CONVERTED TO A NAPIER 'ICE WAGON'.

21 : SOME ASPECTS OF HIGH SPEED FLOW (PART II), *by V. T. Forster, B.Sc.(Eng.), A.M.I.Mech.E., Head of the Air Flow Laboratory, Steam Turbine Division.*

34 : THE APPLICATIONS OF ANALOGUE COMPUTORS IN THE DEVELOPMENT OF GUIDED WEAPONS, *by R. W. Williams, B.Sc., Ph.D., A.Inst.P., Guided Weapons Division.*

All communications respecting Editorial Contents should be addressed to the Editor, THE ENGLISH ELECTRIC JOURNAL, THE ENGLISH ELECTRIC COMPANY LIMITED, STAFFORD, ENGLAND.

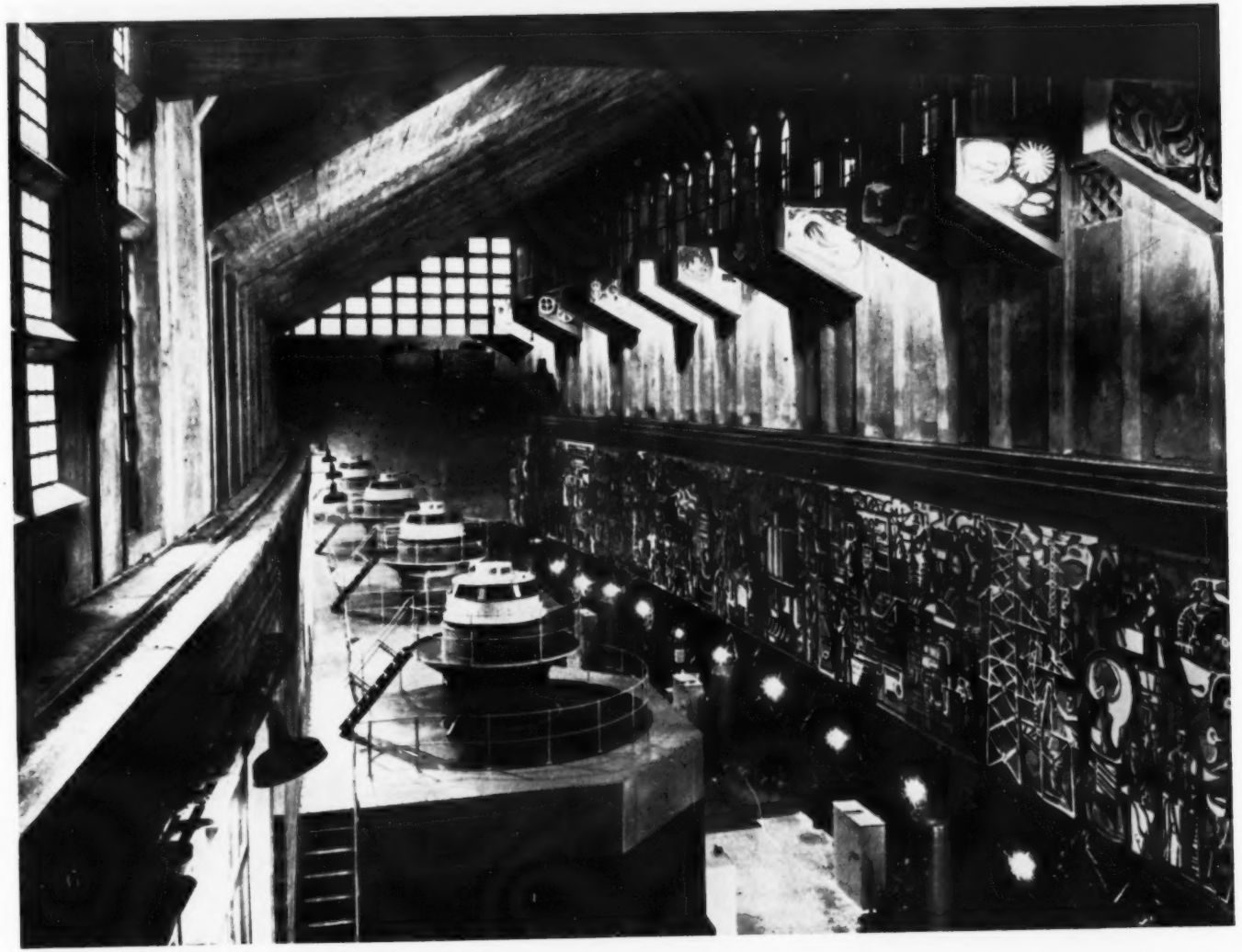

Interior of Salime power house, showing the four 35,000 kVA generating sets

Salime Hydro-electric Power Station in Spain

By H. S. POUND-CORNER, M.A., A.M.I.E.E.

THE SALIME POWER STATION was built and is operated by Saltos del Navia en Comunidad, a subsidiary organisation created by the two companies Electra de Viesgo S.A. and Hidroelectrica del Cantabrico S.A. with headquarters respectively at Santander and Oviedo, for the exploitation of the hydro-electric resources of the River Navia in Northern Spain. This river has its source in the mountainous district between Lugo and Ponferrada and flows northwards to enter the sea at a small fishing village, also called Navia, situated about 90 kilometres west of the port of

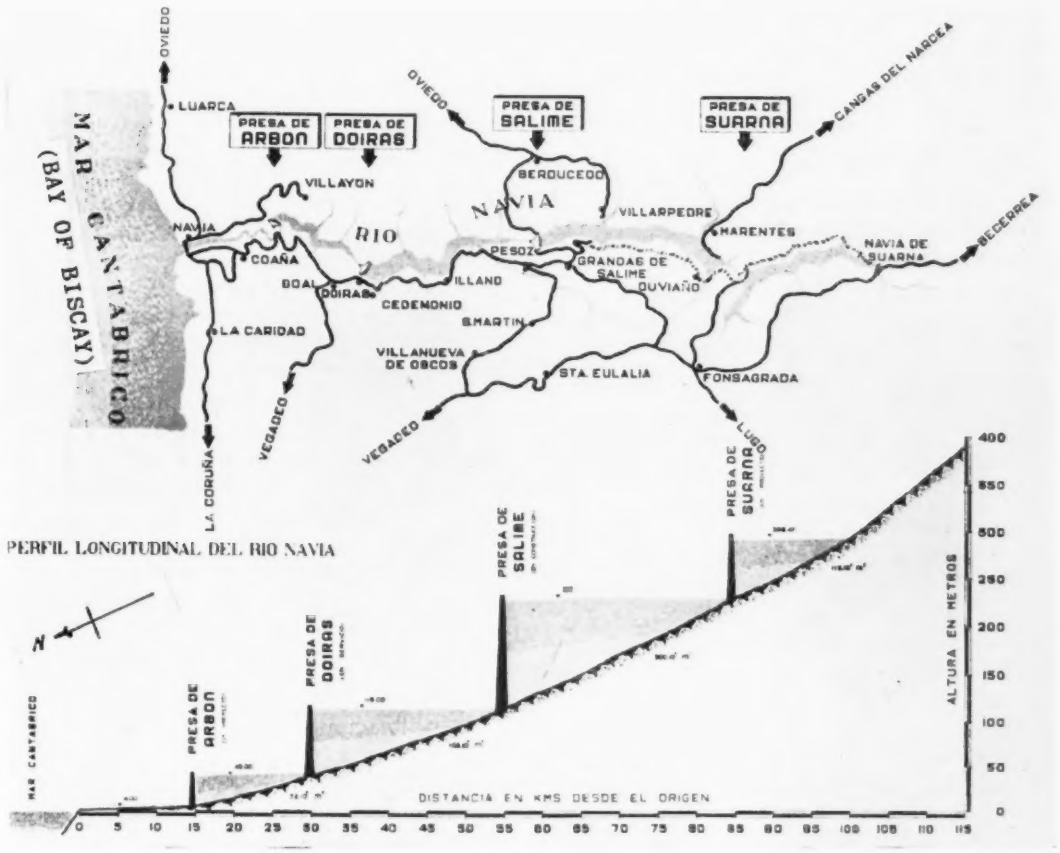

Fig. 1.—Geographical layout of the river Navia project

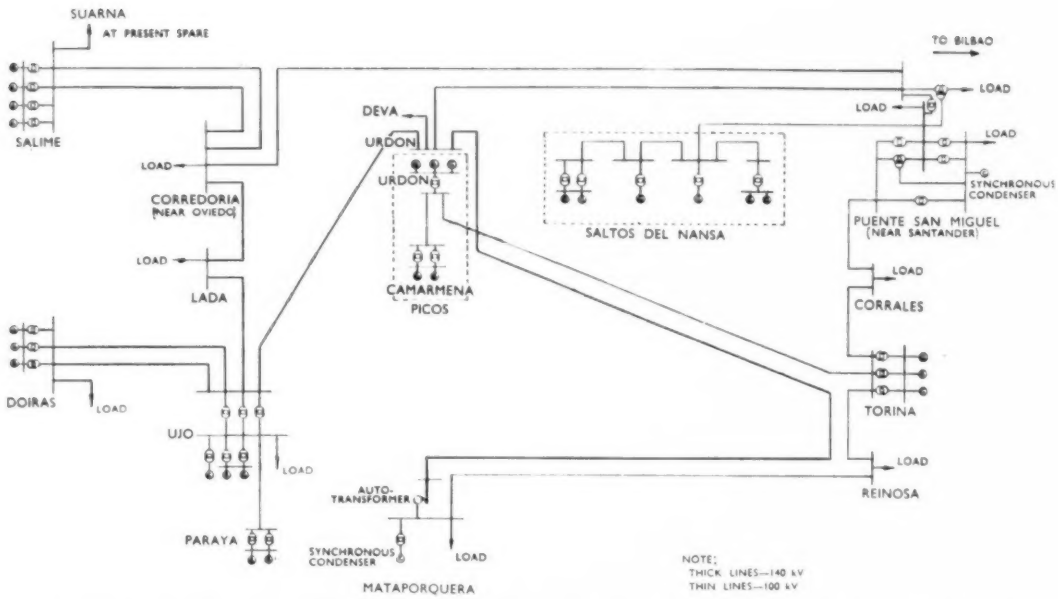

Fig. 2.—140 kV system fed by Salime and the other hydro-electric power stations on the river Navia

Gijon where most of the plant and equipment for Salime was landed.

Fig. 1 shows the geographical layout of the complete project and it will be seen that the full development of the river provides ultimately for five stations, namely :—

(*a*) Doiras, which was built by Electra de Viesgo in 1934 and contains three sets each of 20,400 metric h.p., 18,000 kVA.

(*b*) Salime, at Grandas de Salime, containing four sets each with a maximum output of 50,000 metric h.p. The generators are each rated at 35,000 kVA. This station was inaugurated by General Franco in August 1955.

(*c*) Silvon, now in course of construction below the Doiras dam and which will contain initially one set of 44,750 metric h.p., 35,000 kVA, space being left for a second similar set to be added later.

(*d*) Suarna, upstream from Salime, the project for which is nearing completion.

(*e*) Arbon, downstream from Doiras, which, when built, will complete the exploitation of the river Navia.

The English Electric Export and Trading Company was awarded the contract on the 1st January 1949 for the supply and erection at Salime Power Station of the four main turbine inlet valves, the four main vertical Francis type turbines with their draught tubes and auxiliary equipment, the four main alternators, the four main transformers, all the 380 volt auxiliary switchgear, the 11 kV interconnecting switchgear, the 140 kV main switchgear and the 11 kV power cables between the alternators and the 11 kV cubicles.

Orders were placed with Spanish firms for the supply of the four main penstocks each with an inlet butterfly valve, the two scour valves with their penstocks, the draught tube stoplogs, the four 11kV/380 volt unit transformers, all the remaining power and control cables, the main 150/25 metric ton main station travelling crane, the 75 ton crane for the transformer house and other cranes.

The first set at Salime was commissioned on the 20th December 1953, and, as mentioned previously, the official inauguration of the completed station by General Franco took place in August 1955. Subsequently, in November 1955, The English Electric Company was awarded a contract for similar plant

and equipment for Silvon Power Station, and this is described briefly later in this article.

The load centres (Fig. 2) normally fed at 140 kV by Salime and the other stations on the Navia are (*a*) the mining and industrial areas in Asturias around Oviedo and Ujo, including a very large steelworks being constructed at Aviles, near Gijon, for which The English Electric Company is supplying three large rolling mill drives, totalling over 20,000 h.p., with extensive auxiliary equipment, and (*b*) the mining and industrial areas inland from the city of Santander. In addition, there is a link between Santander and Bilbao, by means of which power can be supplied to Bilbao when necessary. Synchronous condensers are installed at Puente San Miguel and at Mataporquera. A 140 kV link also exists between Doiras and Lugo in the west.

The approach to Salime in the early stages was sometimes difficult, or at least tedious, because of the nature of the terrain. The construction camp had to be built on the west or left bank of the river, which is on the far side from Oviedo, where the headquarters of the construction company, Saltos del Navia en Comunidad, is situated. The route from Oviedo to Salime therefore passed through the villages of Navia and Doiras. This journey took about four hours and in winter the road between Doiras and Salime was sometimes blocked by snow. It was very doubtful if the road from Navia to Salime, via Doiras, could possibly have been improved sufficiently to stand the very heavy traffic required. Later a bridge was built which very much improved communications with Oviedo. The limits for transport to site were fixed at 47 tons, or 5 metres wide by 4 metres high.

In order to overcome some of these difficulties of approach, Saltos del Navia built a ropeway some 37 km long with a capacity of 35 tons/hour between the village of Navia and Salime. This was used primarily, and most successfully, for the transport of cement, sand and aggregate for the dam, but it was also used at times for other things such as food and fuel when the road from Doiras was blocked by snow. It is interesting to note that due to the difficulties of the terrain the road from Navia to the power station site is no less than 77 km compared with 37 km for the ropeway.

The Dam

The Salime dam (Figs. 3, 4 and 5) is of the arch-gravity type, having a uniform triangular section

Fig. 3.
The Salime reservoir, dam and spillway

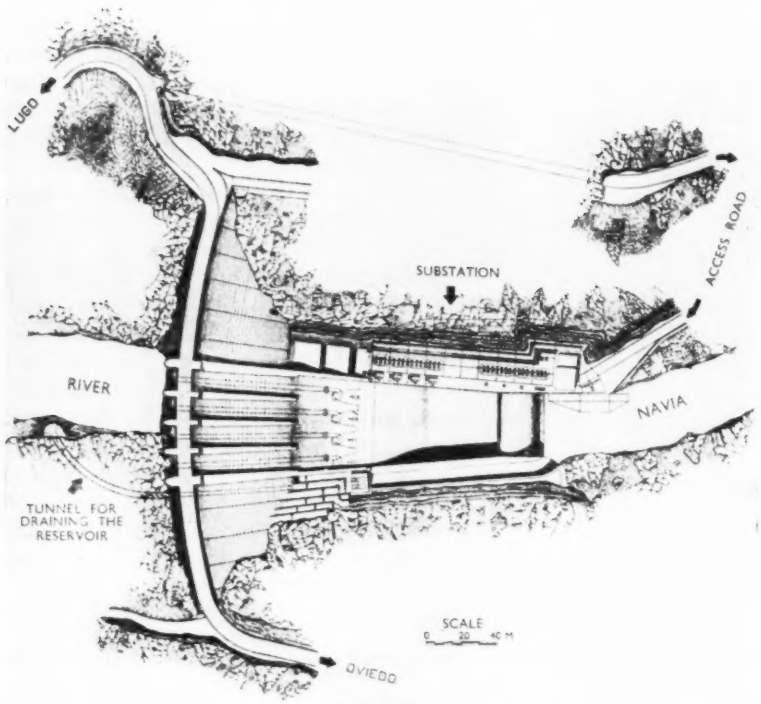

Fig. 4.—Plan layout of the Salime dam and spillway

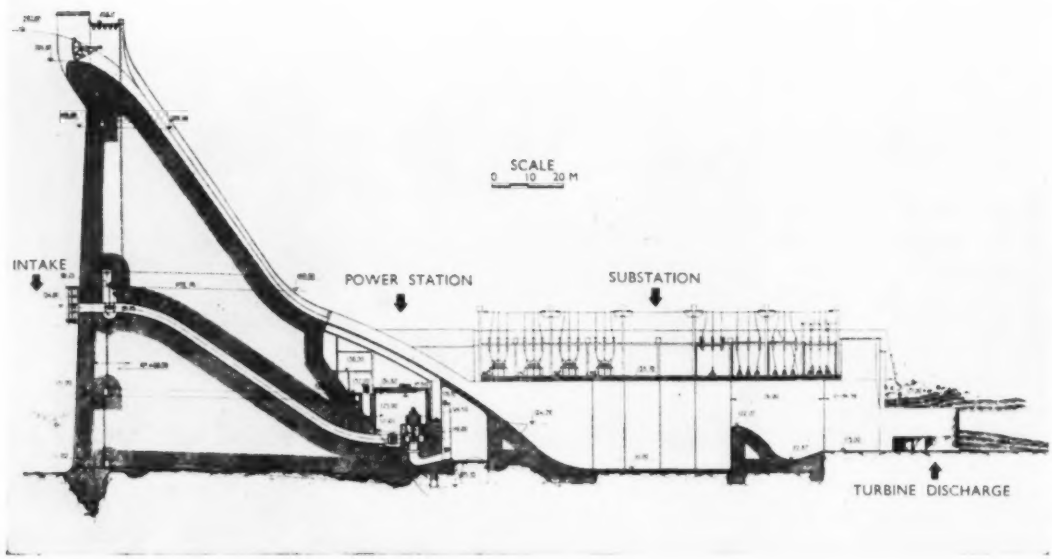

Fig. 5.—Vertical section through dam, power house and spillway

throughout its length, the slope of the upstream face being 5% and that of the downstream face 72%. The crest lies on a curve of 400 metres radius and its height above the foundation is 131·5 metres. The horizontal length of the crest is 250 metres and its width is 9 metres.

The four penstocks for the four turbines lie embedded throughout their entire length in the structure of the dam. They are each about 90 metres long and have an internal diameter of 2·5 metres. Each pipe has an intake screen, and the intake is controlled by a butterfly type valve, to which access is obtained through a gallery in the dam, as indicated in Fig. 5. Each penstock connects at its bottom end with an 'English Electric' Straightflow valve of 2130 mm diameter which admits water to the turbine.

For scouring and draining the reservoir, the water is led through a 3 metre diameter tunnel as far as the upstream face of the dam where it feeds into a 2 metre diameter penstock embedded in the dam throughout its length. This penstock has stoplogs at the intake, and at the bottom end it divides into two branches, each of which has a sluice type valve in series with a balanced Larner-Johnson type valve.

Fig. 6.—Looking downstream from the dam crest, showing spillway, stilling basin and, on the left, the substation containing the main switchgear and transformers

The Power Station and the Spillway

The design of Salime hydro-electric power station is very interesting for several reasons, but mainly because of the unusual design of the spillway, which flows over the roof of the power station into a stilling basin downstream from the tailrace chamber (Figs. 6 and 7).

To enable the necessity for this to be appreciated it should be explained that the river Navia flows for the most part in a deep valley running through high mountains and is fed by melting snow as well as by springs and rainfall. The total catchment area is 1,806 sq km, and the average flow at Salime is 51 cubic metres per second. The river is very short, judged by Spanish standards, being only 115 km long, but in this distance it falls 400 metres. Under such conditions severe floods are to be expected at times, and the Salime spillway had to be built for a maximum flow of 2,000 cubic metres per second, equivalent to dissipating about a million horsepower under conditions of maximum flood. This must be done in a very narrow valley where there is danger of landslides, or even avalanches in winter, due to the steep inclination (about 45°) of the strata and the slaty nature of the rock.

As there was not enough room for the power station and spillway side by side at the foot of the dam, it was decided to put the power station at the foot of the dam and carry the spillway over the

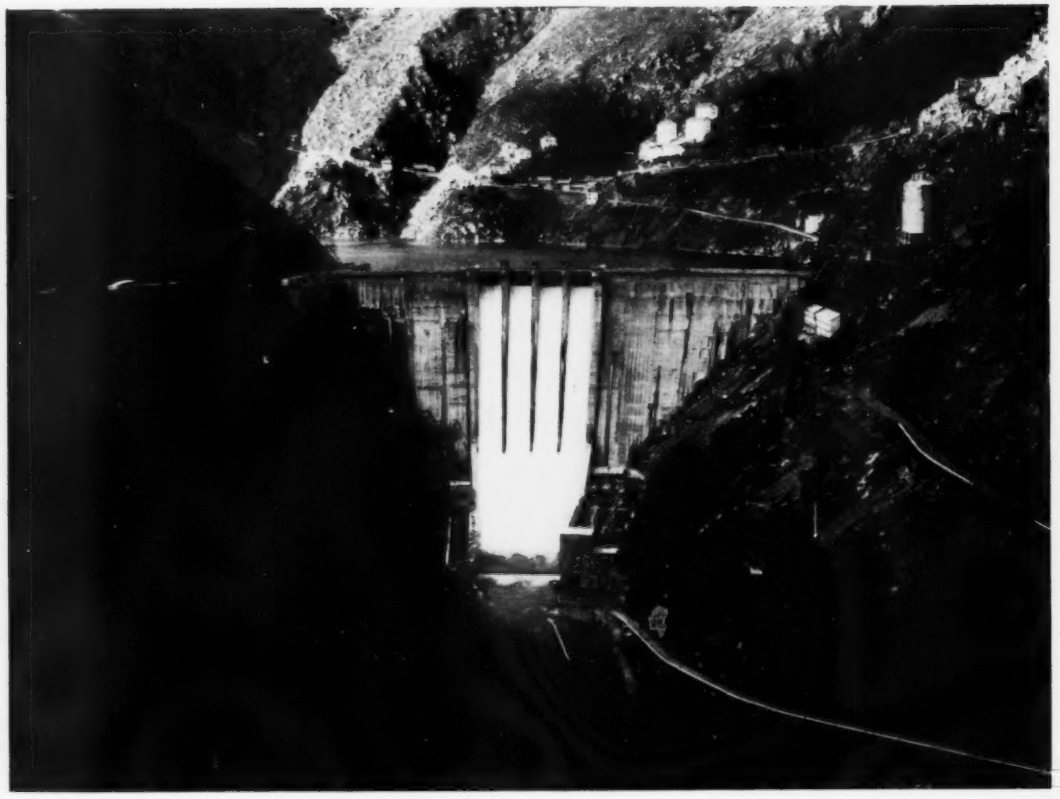

Fig. 7.—The Salime dam and spillway

station roof to discharge into a stilling basin, instead of using a ' ski jump ', in order to reduce the spume, spray and reverberation to a minimum. This necessitated carrying away the tailrace waters from the turbines by a tunnel, which is not under pressure, feeding back into the river just downstream from the stilling basin.

The spillway (Figs. 3 and 5) is controlled by four sector gates, each 12 metres wide and 7 metres deep, separated by three pillars, each 4 metres wide. From these pillars three tapering ribs run down the spillway to a point just upstream of the power station (Fig. 7), where the four separate streams merge into one. The overall width of the four streams at the dam crest is $4 \times 12 = 48$ metres, at the bottom of the spillway 40 metres, and at the downstream end of the stilling basin 35 metres. The stilling basin is 11 metres deep.

This slight narrowing of the waterway towards the bottom tends to maintain stable conditions as the water gathers speed during its descent from the dam crest to the stilling basin. In particular it helps to avoid cavitation of the floor of the spillway and to prevent the formation of dangerous transverse waves in the water. There is no ' ski jump ': the water simply slides into the stilling basin and flows along its bed until it is turned back on itself by the downstream retaining wall (Fig. 5) so dissipating its energy. A row of ' dragon's teeth ' is located at the point where the spillway and stilling basin meet, in order to aerate the water before it enters the stilling basin. This prevents cavitation of the floor of the basin. The profile of the spillway is not a continuous uniform gradient. It has been shaped to give a very slight lift to the water as it passes over the power house in order

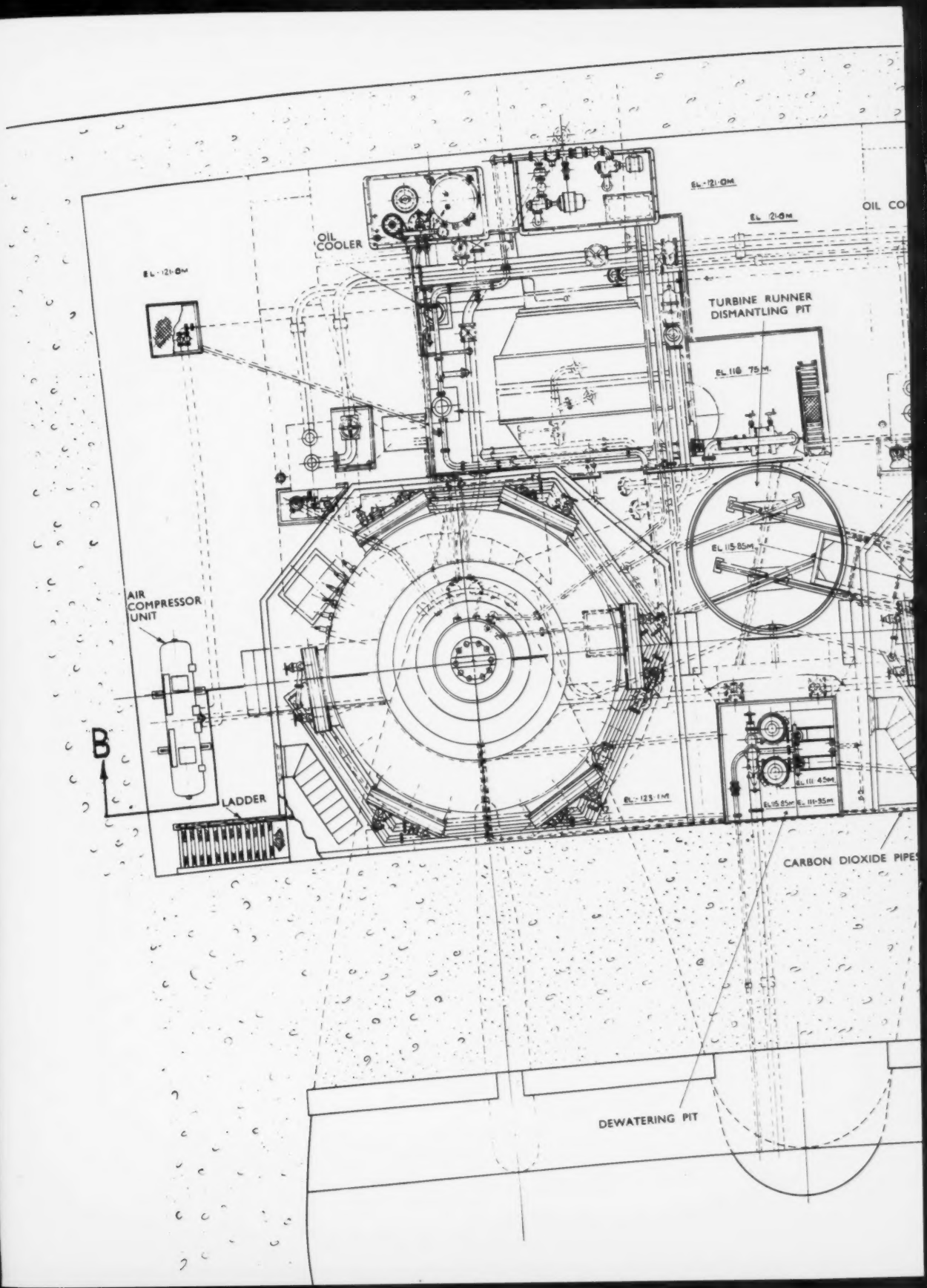
EL.-121·0M
OIL COOLER
EL.-121·0M
EL 21·0M
OIL CO
TURBINE RUNNER DISMANTLING PIT
EL 116 75M.
EL 115·85M.
AIR COMPRESSOR UNIT
B
LADDER
EL.-123·1M
EL 111 45M
EL 115·85M EL. 111·35M
CARBON DIOXIDE PIPES
DEWATERING PIT

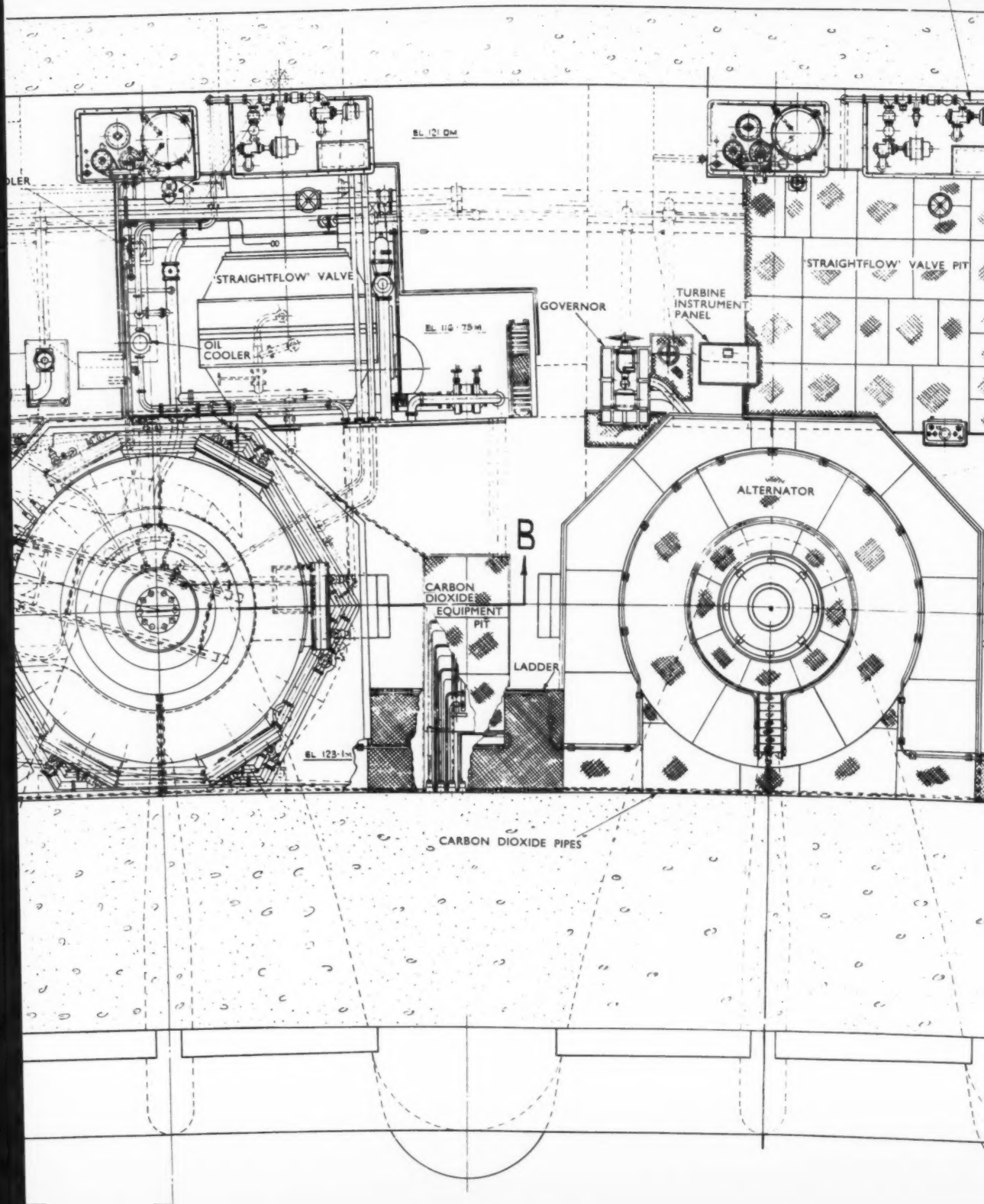

Fig. 8.—Plan view of the power house

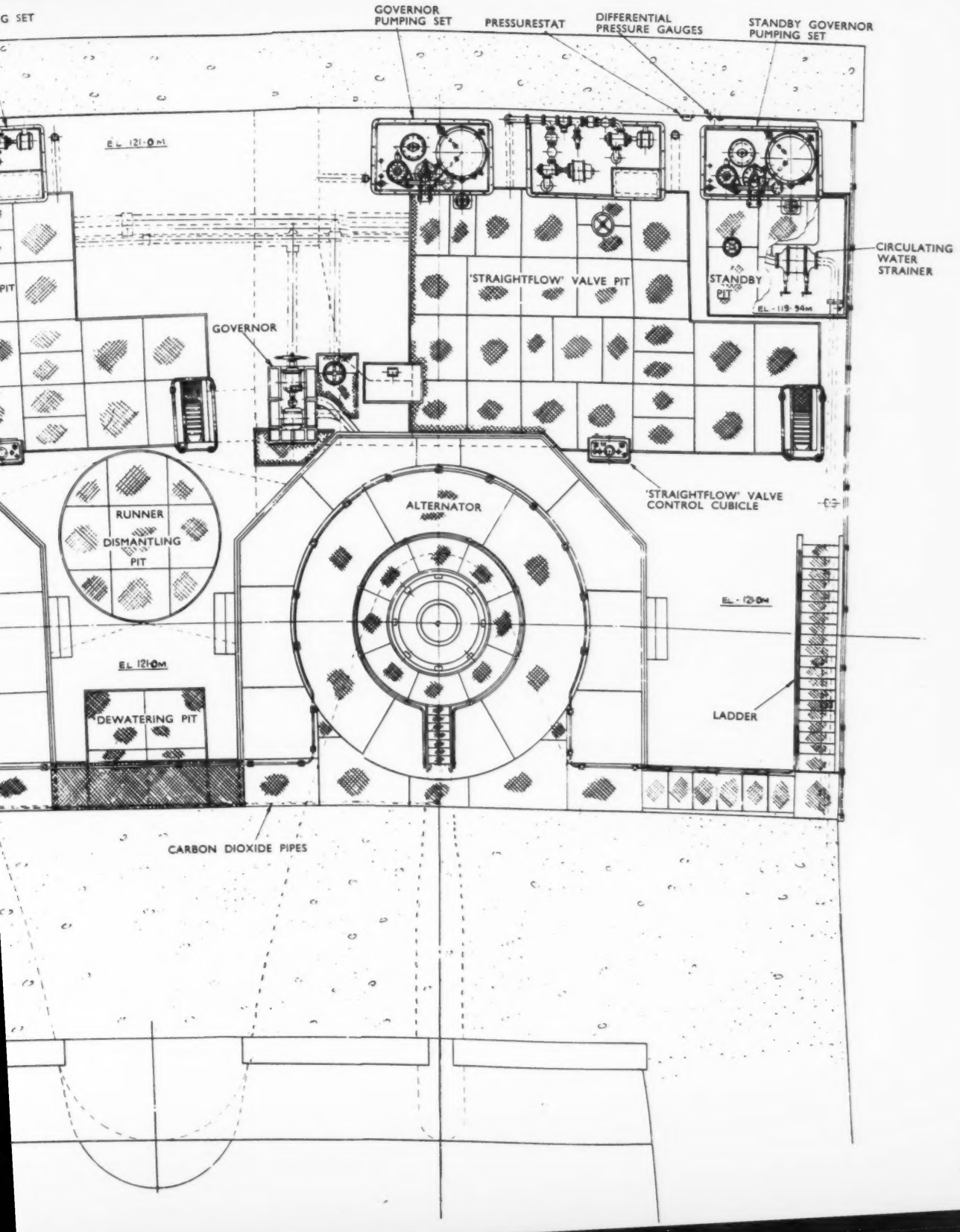
G SET
GOVERNOR PUMPING SET
PRESSURESTAT
DIFFERENTIAL PRESSURE GAUGES
STANDBY GOVERNOR PUMPING SET
EL 121·0M
CIRCULATING WATER STRAINER
'STRAIGHTFLOW' VALVE PIT
STANDBY PIT
EL - 119·94M
GOVERNOR
'STRAIGHTFLOW' VALVE CONTROL CUBICLE
ALTERNATOR
RUNNER DISMANTLING PIT
EL - 120·0M
EL 121·0M
DEWATERING PIT
LADDER
CARBON DIOXIDE PIPES

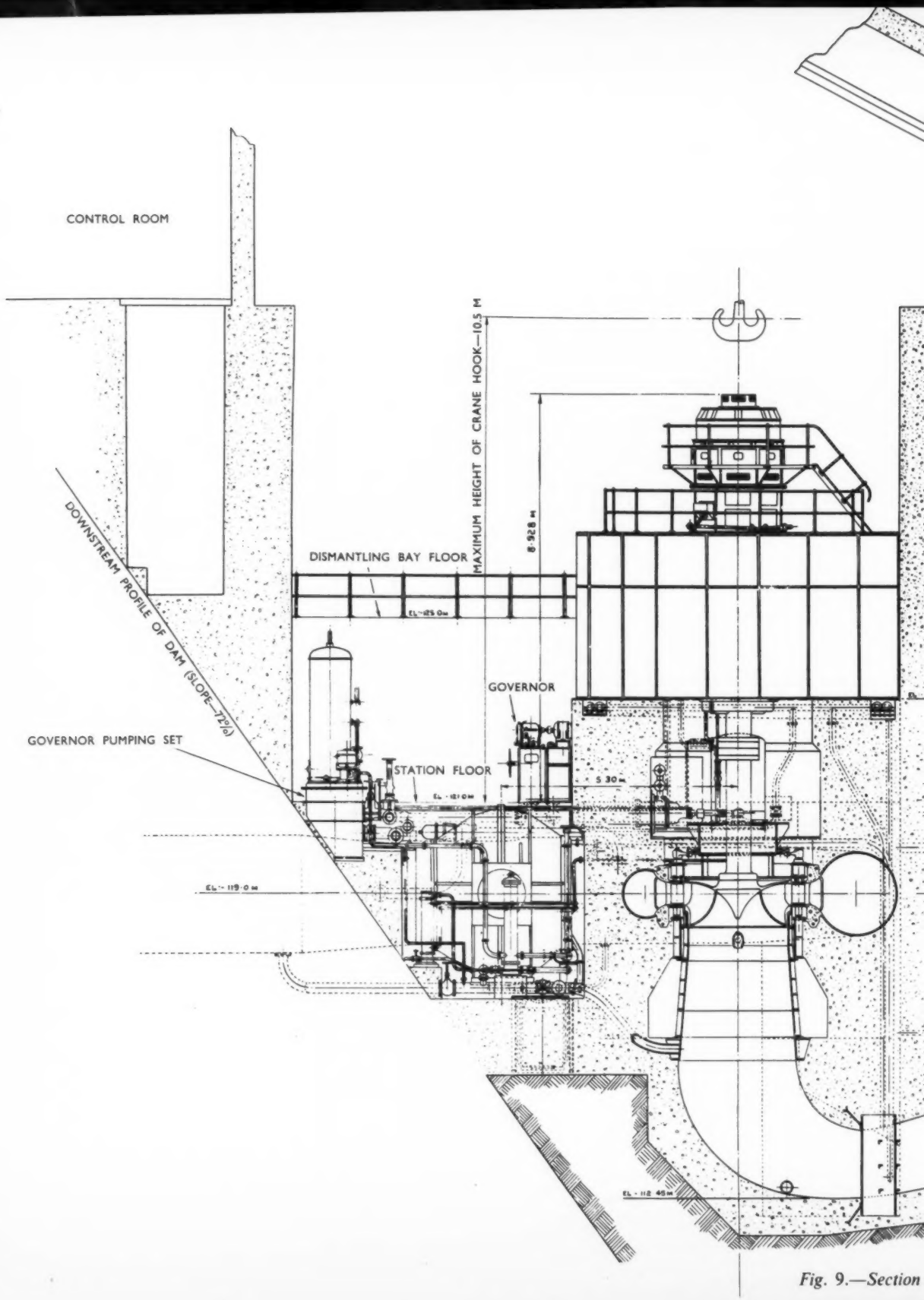

Fig. 9.—Section

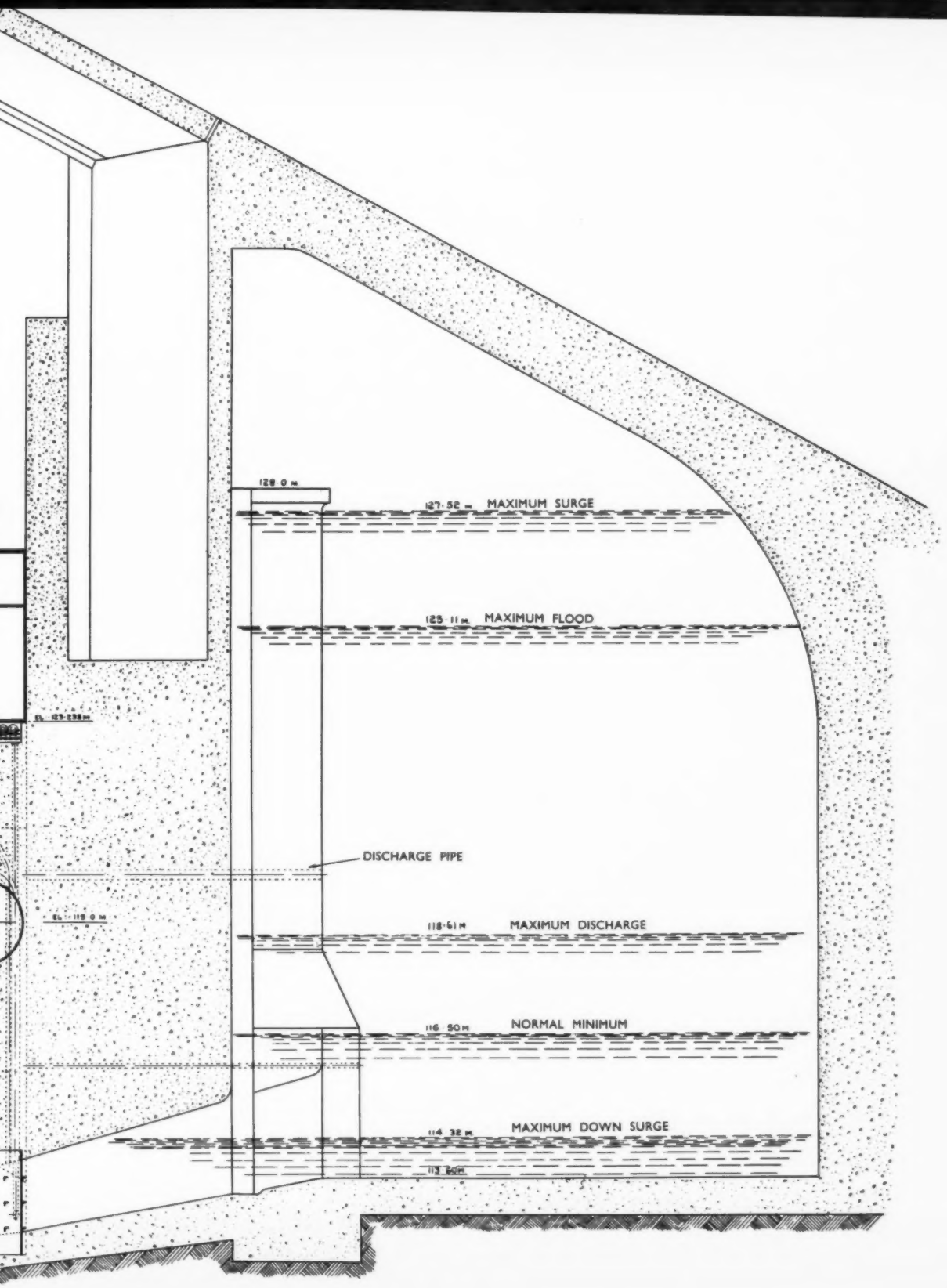

Section through one of the turbines, showing exterior of alternator

to relieve to some extent the pressure at that point.

Another important feature is that if a horizontal section of the spillway is taken at any point the surface is not a straight line but a slight curve conforming to the curvature of the main dam. For this reason the four main sets in the power house are located on an arc of 310 metres radius instead of having a straight longitudinal axis as is usually the case. Consequently, the station overhead travelling crane rides on a curved track (Frontispiece) and has larger diameter wheels on the upstream end than on the downstream to compensate for this curvature.

As will be seen in the vertical cross-section of the dam and power house (Fig. 5), a bridge consisting of steel girders spans the space between the face of the dam and the downstream wall of the power house, in order to raise the spillway sufficiently to provide room for the power house etc. underneath it. Three main transverse bays are provided. The power station itself occupies the middle bay, and the bottom one houses the tailwater chamber. The upstream bay was originally intended to house the main 11/140 kV transformers, in addition to the control room and usual offices, but as this involved running four 140 kV lines from the transformers to a substation located about a kilometre away at a suitable point on the hillside, considerations of space and protection ruled it out. Consequently, a platform of sufficient size to house the four main transformers, as well as the 140 kV switching station, was made alongside the stilling basin on the left bank of the river (Figs. 6 and 12).

The water in the tailrace chamber passes through a free flowing tunnel of 7 metres internal diameter, running underneath the substation, and discharges into the river just downstream from the counter-dam of the stilling basin, thus ensuring stable tailrace conditions for the turbines.

Layout of the Power Station

The layout of the power station can be seen in Figs. 8 and 9. It follows the normal 'English Electric' one-floor arrangement, in which all parts of the equipment and plant, including the main valves, come under direct access of the crane. The floor is located at an elevation of 121 metres above sea level and the turbine centre line is at 119 metres. The spiral casings and draught tubes of the turbines are completely embedded in the concrete foundations, below the floor level.

Each alternator stator is supported on a reinforced concrete cylindrical plinth which rises direct from the main foundations through the floor and continues to the height of the soleplates on which the alternator stator and lower bracket rest. This concrete plinth is designed, with a liberal margin, to carry the dead weight of the alternator stator and all rotating parts, plus the hydraulic thrust and any torsional stresses which may arise in operation. Arched access openings are provided in this plinth, at the turbine floor level, to permit inspection of the turbine regulating gear etc. whilst the set is running. Equipment for the control and metering of the turbine/generator unit is disposed conveniently on the station floor, adjacent to the plinth.

The curvature of the longitudinal horizontal axis of the turbines, to which reference has been made, can be seen in the Frontispiece and Fig. 8. It was necessary to make the width and height of the power station as small as possible, so that the spillway could be kept as low as possible, and a considerable saving in these dimensions was obtained by adopting this curved plan.

Two other important departures from standard design were made in order to keep to a minimum the crane hook height for lifting the rotor out of the stator: the turbine-alternator shaft was divided into three sections instead of the usual two, and the pilot exciter was partly telescoped inside the main exciter.

An important consideration when endeavouring to keep the height and width of the station to a minimum was that under no circumstances was it permissible to encroach on the 72% downstream profile of the dam.

The resultant arrangement can be seen in the Frontispiece and Fig. 9, which show how the spillway passes over the four generating sets. What is actually visible in the machine room is not the spillway channel itself but an apron placed between the spillway and the power station in order to collect any seepage water from the spillway and drain it away into the tailrace chamber, thus keeping the machine room dry.

Provision has been made for dismantling the turbine runner from below by making the throat of the turbine draught tube removable, so that the runner can be lowered on to a special truck and then run out on rails to a pit, where it comes directly under the crane. A major maintenance overhaul of the turbine can thus be made without disturbing the alternator in any way. There are two de-watering pits, one to each two machines, and in addition provision is made to empty the penstock, with the main turbine valve closed, by means of a pipe which by-passes the valve and discharges direct into the draught tube. Any residual water in the spiral casing, or in the valve, can also be drained off into the draught tube, once the penstock is empty, by connecting the bottom of the valve casing to the by-pass pipe.

Turbine Inlet Valves

The main turbine valves are of the 'English Electric' Straightflow type, having a bore of 2,130 mm and a double seal. They are operated by water pressure, and are designed to close against the maximum flow in emergency.

The valve consists of a main body of spherical form, made in halves of electrically welded mild steel, and a cylindrical inner body which acts as a prolongation of the pipeline. The valve door is hemispherical and has a solid section which closes the pipe bore, and a pierced section which coincides with a gap in the main body and so continues the smooth pipe bore when the valve is open. When the valve is shut, leakage is prevented by a rubber seal which is forced by pipeline water pressure against a stainless steel surface on the door. In addition, there is a second rubber seal which can be used when it is necessary to inspect or replace the main rubber seal, without emptying the water in the pipeline. The Straightflow valve is normally operated from its own control panel on the turbine room floor, but in emergencies it can also be closed by remote control from the main control room.

This design of valve possesses the advantage of presenting a straight and smooth pipe bore to the water when open, but is always capable of closing safely in emergency because the hemispherical door cuts through the water without deflecting it. Water hammer is avoided by regulating the movement of the valve operating servomotor by means of a travelling control screw which progressively diminishes the speed of closing.

The Turbines

The four main turbines are of the vertical Francis reaction type running at 300 r.p.m., each giving a maximum output of 50,000 h.p. under a net head of 112·5 metres. The minimum working net head is 69 metres under which conditions the turbine gives 21,000 h.p.

The vertical section of the assembly of one of the turbines is shown in Fig. 9. The variations of the tailwater levels under different conditions can also be seen in this drawing. The spiral casing was welded to the speed ring in the works and then the whole assembly was divided into four parts for transport to site, where they were finally bolted and welded together, and tested, before being embedded in the concrete foundations. The runner is fabricated and not cast, the runner blades being of stainless steel formed to shape before being welded to the runner crown and skirt, and, as already stated, the complete runner can be dismantled and replaced from below without disturbing the alternator above it. It has steel labyrinth water sealing rings. The guide vanes and their trunnions are of mild steel.

The main top cover of the turbine is of box construction of electrically welded steel and it is provided with flanges and seatings for (*a*) the housing for the main turbine shaft water seal, which is of the carbon segment type, (*b*) the housing for the main turbine bearing, (*c*) the housings for the gunmetal bushed bearings of the guide vane trunnions, and (*d*) facings for the regulating ring. This ring is of welded steel, with gunmetal gliding pads, and is provided with cast iron guide vane levers and links, and two steel rods directly connected to the pistons of the operating servomotors.

The turbine bearing consists of a welded steel housing, in halves, bolted and dowelled to the turbine cover, and a cast iron bush, also in halves, lined with anti-friction white metal. There are two pumps for the lubricating oil, one driven by an a.c. motor and the other, used as a standby, driven by a d.c. motor. The standby unit is brought into service by means of an oil flow relay on failure of the a.c. motor-driven pump.

The governor follows the usual ' English Electric ' principle : the actuator is driven by a pendulum motor, and incorporates a speed adjustment device for synchronising and loading, and an underspeed device. It controls an oil-operated pilot servomotor which is itself fitted with a device for shutting down due to overspeed, low oil pressure, the operation of the electrical protection, or by push button from the control room. The pilot servomotor in turn operates the main distributing valve which controls the oil to the twin guide vane servomotors.

Each governor unit is supplied with pressure oil from its own pumping set and receiver. In addition the four pumping sets are inter-connected, by means of bus pipes, with the standby pumping set, which cuts in when the oil pressure falls below a pre-determined value.

The Alternators

The four main alternators are designed to give an output of 35,000 kVA each at 0·9 power factor 11,000 volts 3-phase 50 cycles, the speed being 300 r.p.m. The machines are of the vertical shaft two-bracket type, a combined thrust and guide bearing being mounted on the upper bracket above the rotor, and a second guide bearing on the lower bracket below the rotor.

The stator frame was divided into two parts for transport to the site, and the winding is of the two-layer basket type with conductors built up of laminated copper, the insulation being Class B in accordance with B.S.226. Temperature detectors are embedded in the winding, and an indicating instrument, with an alarm for excessive temperature, is provided.

The rotor was assembled at site by shrinking the steel hub packets on to the shaft and then fitting the salient poles on the hub. Both the poles and the hub are dovetailed and fitted with taper side keys in the slots in the rotor hub to facilitate removal for repairs.

The generators have closed-circuit cooling, the air being circulated by fans attached to the rotor and cooled by six water-cooled air coolers arranged tangentially outside the stator frame, instead of radially, so as to reduce the overall diameter as much as possible.

A governor alternator is mounted on the extension shaft directly above the thrust bearing, to supply a synchronous motor which drives the turbine governor actuator pendulum. The main and pilot exciters are mounted on the same shaft, above the governor alternator, their fields being controlled by an automatic voltage regulator, with the requisite switchgear.

The whole dead weight of the revolving parts, plus the vertical hydraulic thrust, is carried on a thrust bearing of the pivoted pad type, mounted on the upper bracket, the load being transmitted through a thrust collar which is lightly pressed on to the shaft and secured by keys. The pads are pivoted to enable them to tilt freely in any direction, and are also independently adjustable to ensure that each carries the same load. The upper

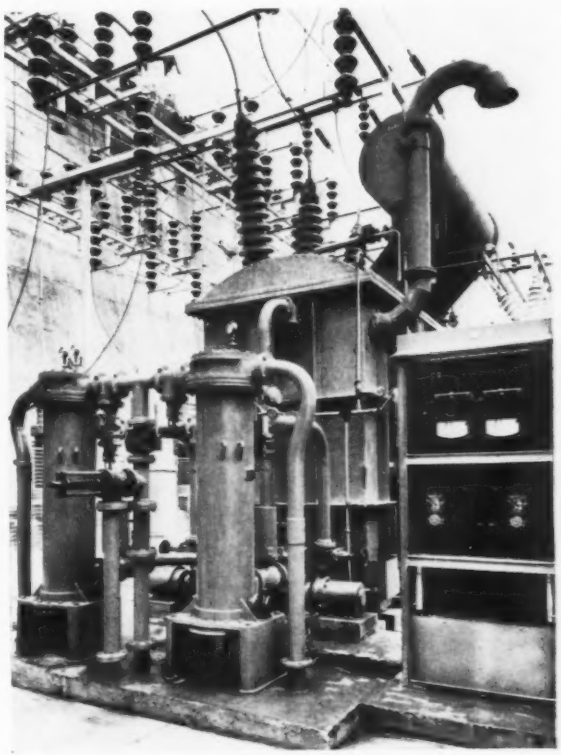

Fig. 10.—*One of the four main generator transformers, showing the two oil-water heat exchangers*

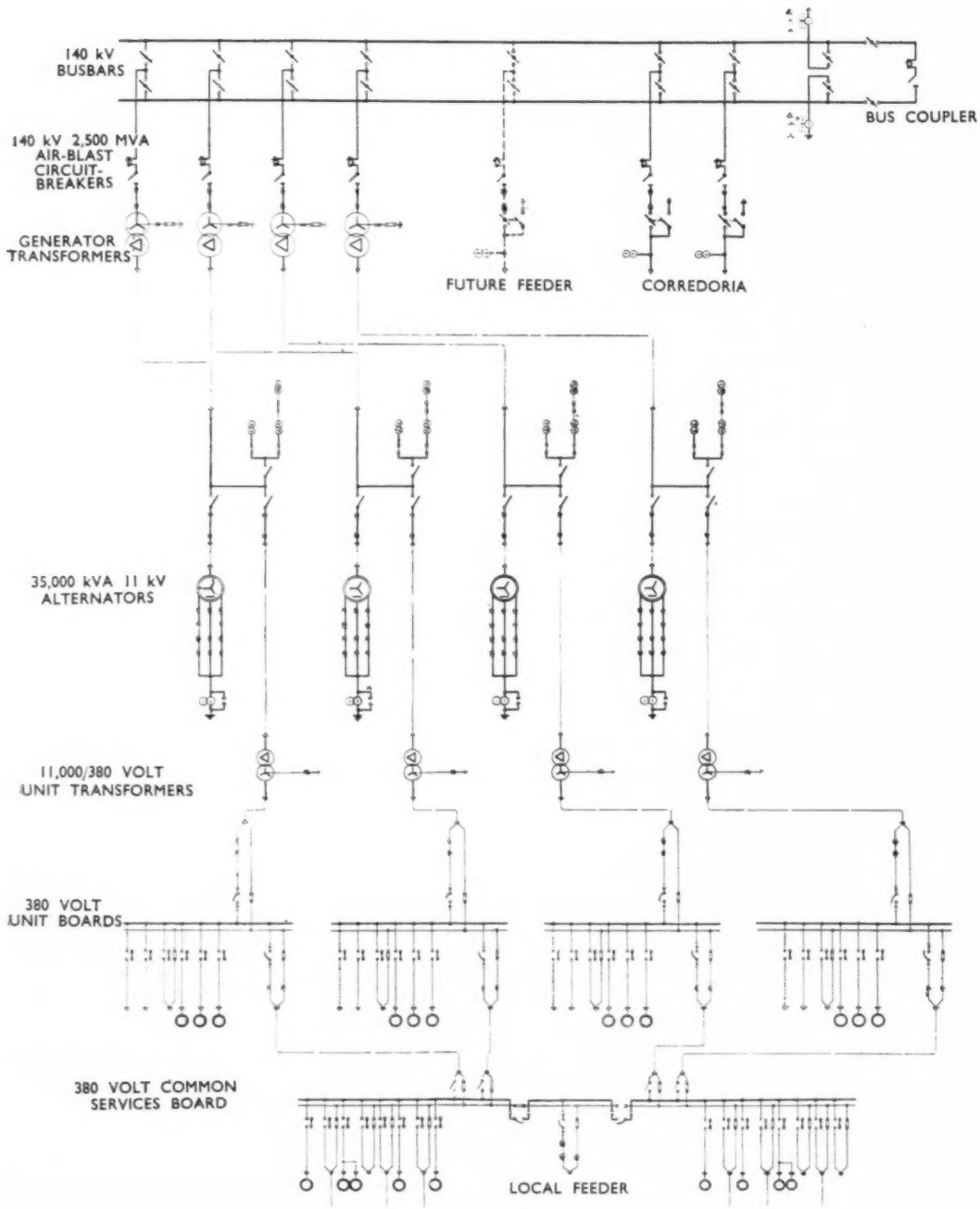

Fig. 11.—*Main electrical connections at Salime*

guide bearing also has pivoted pads, which run on the polished vertical surface of the thrust collar. Both bearings run in a common oil pot through which the oil is circulated by an a.c. motor-driven pump, with a d.c. motor-driven pump acting as a standby. A second guide bearing, also of the pivoted pad type, is mounted on the lower bracket, below the rotor, and this is included in the same lubricating system as the combined thrust and upper guide bearing.

Each of the arms of the lower bracket carries a braking and jacking cylinder supplied with compressed air for braking, and oil under pressure for jacking. The brake shoes are Ferodo lined and press against a brake track on the underside of the rotor, which can be brought to rest from full speed in a few minutes. The compressed air equipment consists of two a.c. motor-driven compressors, and the oil for jacking is supplied from a portable hand-operated pump. After jacking, the rotor can be maintained in position by the follow-up screws.

The Transformers

The four main transformers (Fig. 10) are 3-phase units each rated at 35,000 kVA and having a no-load ratio of 11/140 kV, the 11 kV winding being delta connected and the 140 kV star connected. Advantage has been taken of the fact that the neutral point of the system is solidly earthed to provide graded insulation on the 140 kV windings, with tapping points connected in the neutral end of the high voltage coils to give $\pm 2\frac{1}{2}\%$ and 5% voltage variation. The tap-changer is manually operated from the exterior of the tank, and is padlocked to ensure that it is only operated by a responsible engineer.

As can be seen in Fig. 10 each transformer is cooled by means of two oil-water heat exchangers, each of which is adequate for continuous full load operation. Provision is made to change over from one cooler to the other without interruption of the circuit or change of load. The oil is circulated by means of a pump, which keeps the oil pressure in the cooler above that of the water to ensure that in the event of leakage there shall be no risk of the oil becoming contaminated with water.

The transformers are of the core type, each contained in a fabricated mild steel tank suitably reinforced to permit handling during the journey to site and subsequently when filled with oil. The yokes are clamped by fabricated steel frames and the legs are secured by a single row of bolts from which the pressure is distributed over the face of the limbs by a series of short steel pads: both the bolts and the pads are insulated from each other and from the core. Each completely erected unit, comprising core and windings, was dried out in a vacuum tank and impregnated with hot transformer oil.

The unit transformers were manufactured by a Spanish company and are rated at 800 kVA each, the no-load ratio being 11,000/380 volts. Each is capable of supplying the unit auxiliaries for four alternators, plus all the common services of the station.

Switchgear for 11kV and 380 volts

The key diagram of Salime Power Station is shown in Fig. 11 and it will be seen that the unit arrangement has been adopted, in which each set normally runs independently of the others and supplies its own auxiliaries by means of a unit transformer connected direct to the alternator.

The 11 kV switchgear consists of isolators housed in cubicles for isolating each alternator from its main transformer and also for disconnecting the feed to the unit transformer if desired.

With the exception of the governor oil pump, alternator and turbine main lubricating oil pumps and the alternator heaters, all the main machine auxiliaries and other station and local services are supplied at 380 volts from the common services board which is fed from any one of the four 380 volt unit boards. These three oil pumps and the alternator heaters for each set are supplied direct from the unit board of the set. The unit boards and the common services board consist of air-break draw-out type circuit-breaker units and 'Combination' fuse-switch units. There is at present no auxiliary generating set to provide an alternative supply to the common services board although provision has been made for such a supply to be connected to this board if considered desirable at a later date. A 380 volt supply is always available as long as one set is running. If the station shuts down completely it can be restarted by isolating the alternator of one of the sets and feeding from the 140 kV busbars through a

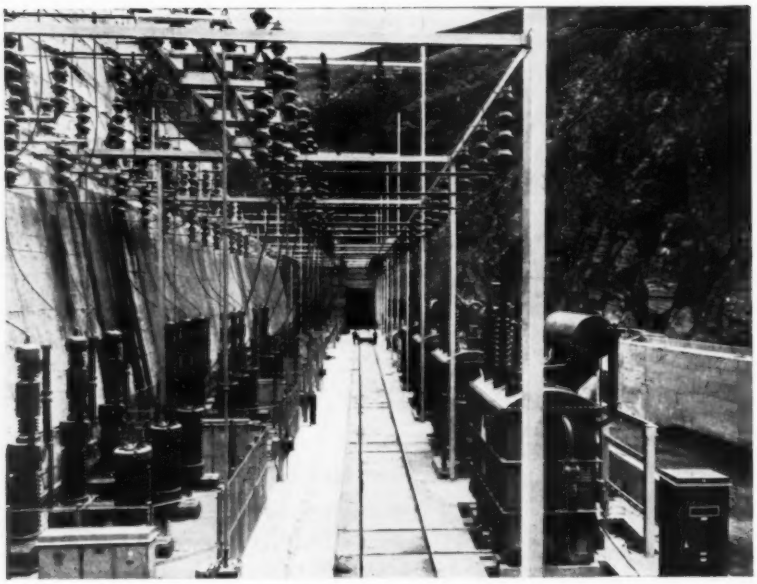

Fig. 12.
The outdoor substation

main transformer and then through the corresponding unit transformer to the unit board of the set, and from there to the common services board of the station.

The whole of the 380 volt equipment, as well as the main control, metering and relay boards for the station, is housed in the bay immediately upstream from the turbine room, from which position the engineer in charge of the control room has an uninterrupted view of the turbine room.

Fig. 13.—*Paintings on the power house walls*

Outdoor substation

The outdoor substation, as already mentioned, is located on the left bank of the river adjacent to the stilling basin. The lay-out can be seen in Fig. 12. As the site is so narrow it was essential to use a ' high ' arrangement, in which the isolators and busbars are vertically above the circuit-breakers instead of adjacent to them as in a ' low ' station. The station has duplicate 140 kV busbars and there are 8 bays, i.e. four transformer bays, three outgoing feeders of which two go to Corredoria and one is at present spare, and a bus coupler and voltage transformer bay.

The 140 kV circuit-breakers are of the ' English Electric ' air-blast type, with two interrupters in

series per phase, having a breaking capacity of 2,500 MVA. All the feeder breakers are provided with high speed auto-reclose control, and duplicate air compressor sets are installed to provide compressed air for the substation.

The connections between the alternators and the 11 kV cubicles are by means of single-phase cables, and from the cubicles to the main transformers by means of three-phase cables.

Network Analysis

The English Electric Company carried out a network analysis for the whole 140 kV system in order to determine the effect that Salime Power Station would have on the system under various conditions of loading, and whether it was advisable to have a direct 140 kV link between Salime and Doiras. The stability of the system under various fault conditions was also studied.

Duty

Salime Power Station is at present being used as a peak load station and is most in demand during the first three months of the year. It has never yet been short of water.

Mural Paintings

As will be seen in the Frontispiece and Fig. 13, the walls of the power house have been painted to depict the changes that have taken place in the Navia River valley throughout the ages and to illustrate the labours involved in harnessing the river to provide abundant electrical energy for the service of mankind.

SILVON POWER STATION

By raising the height of the Doiras dam by three metres, sufficient head was obtained to justify building a new power station on the opposite bank to Doiras Power Station and drawing its water from the Doiras reservoir. This station, named Silvon, will ultimately house two sets each of 35,000 kVA, the turbines being rated at 44,750 metric horsepower under a gross head of 76·3 metres and a net head of 75·0 metres. The speed is 250 r.p.m. The order was placed with The English Electric Company on 15th November 1955 for the first of these sets together with all necessary auxiliary gear. Silvon Power Station will feed into the existing Doiras substation.

Acknowledgments

Grateful acknowledgment is made to Mr. K. Bamford, technical representative in Madrid of The English Electric Company, and to Mr. A. Wilmot of the Water Turbine Department of The English Electric Company, for much of the information contained in this article.

A Lincoln Aircraft Converted to a Napier 'Ice Wagon'

A LINCOLN BOMBER has recently been converted into a flying 'ice wagon' by the Flight Development Establishment of D. Napier and Son Limited, to increase their research facilities and continue development on various methods of thermal ice protection.

In the development of the Napier Spraymat electric de-icing system*, Napier technicians have built up a wealth of knowledge, not only on actual de-icing but also on the formation of ice under simulated conditions and the flight testing of many types of de-icing equipment. In view of this, the Napier Company has been given the task of performing the flight evaluation trials of the 'hot gas' anti-icing installation employed on the Blackburn Beverley freighter.

For this series of tests, a specimen section of the Beverley mainplane has been installed above the Lincoln fuselage just aft of the mid-upper turret position (Fig. 1). The test section has a span of six feet, a mean chord of eleven feet six inches, and incorporates a four foot length of the Beverley leading edge installation. This assembly is mounted on a pivot post which is supported by a horse-shoe

* *Described in E. E. Journal, December* 1954, *Vol.* 13, *No.* 8, *p.* 353.

Fig. 1.—*The converted Lincoln bomber, showing the water spray mast and Beverley test section*

Fig. 2.—Lucas 2½ therm heater installation in rear fuselage (looking aft) with lagged hot air supply duct passing forward and exhaust duct through rear gun turret

shaped box-section reinforcing member built into the fuselage structure.

To cater for various test conditions, provision has been made for the pilot to control the angle of incidence of the test section during flight between $-1\frac{1}{2}$ and $+10\frac{1}{2}$ degrees. A recent test programme for the Beverley specimen was carried out at a datum altitude of 12,500 ft with ambient temperature levels between −5°C and −30°C. A flight speed of 155 knots I.A.S. with the section at an effective incidence of 5·7° simulated the Beverley 'cruise', and 115 knots at an incidence of 10·8° represented the 'climb' condition.

Hot air for the Beverley leading-edge is provided by a Lucas 2½ therm heater unit installed in the rear fuselage (Fig. 2), fuel being supplied from a 25 gallon tank mounted in the rear of the bomb bay. Air intakes, positioned aft of the test section, supply both combustion and circulating air to the heater, the combustion gases exhausting via an exit duct at the rear of the fuselage. The circulating air mass flow developed by the heater unit varies from between 1·0 to 1·5 lb/sec according to altitude and flight speed. This represents a far greater mass flow of hot air than is required by the comparatively short length of test section in this case, and most of the circulating hot air is exhausted via the exit duct. The hot air required for anti-icing is ducted forward where a variable cold air bleed is added as required to control the temperature.

Ice is formed on the test section by a water spray mast containing 36 nozzles, positioned approximately six feet in front of the leading-edge. Water is supplied from two 60 gallon tanks mounted in the bomb bay, which are pressurised to 50 p.s.i. by a compressor fitted to the port inner engine. A two- stage supercharger fitted to the port outer engine supplies air pressure via an intercooler to the water spray nozzles to obtain the necessary atomisation. By varying the atomising air pressure from between 15 to 20 p.s.i., the size of the water droplets can be adjusted to 20 micron for continuous maximum icing conditions and 30 micron for intermittent maximum conditions.

Windows are fitted in each side of the fuselage directly beneath the test section to enable photographic observations to be made through suitably positioned mirrors. Three visual observation positions are provided, one from the astrodome and two others beneath the test section.

A test observer's station (Fig. 3) with accommodation for two observers contains the instrumentation for the test section, a bank of six flowmeters for measuring the spray nozzle water consumption and a water concentration meter. All the controls and instruments necessary for operating the heater unit, the hot air supply and the spray nozzle water and air supplies, are grouped together and the readings recorded by an automatic observer cine-camera installation. In addition to the

Fig. 3.—Observer's station and main control panel (looking forward). Beyond the horse-shoe reinforcing member is the water droplet sampler and camera-microscope

comprehensive record obtained from the automatic observer, the simulated icing conditions used for each test are sampled by a manually-operated droplet sampler. An ice box is provided to preserve the samples caught on glass slides, and a special camera-microscope permits immediate study and recording of each slide during flight.

The anti-icing installation of the Beverley leading-edge test section is supplied with hot air from the heater unit via a flexible coupling to the main supply duct within the specimen. From this duct the hot air passes forward to the leading-edge and then flows rearwards through corrugations between the inner and outer skins into a compartment from which it is extracted by a rearward-facing louvre in the tip of the test section. Minute pitot and static tubes are installed in the corrugations at various points to measure the flow of hot air through the test section. Due to the relatively small mass flow of hot air required by the test section, air temperatures of 130 to 160°C can be obtained.

To improve the general working conditions for crew members during prolonged icing trials, Napier Spraymat heater panels are positioned at all observer's stations in addition to the standard power supply for electrically-heated flying suits and the aircraft hot air system.

The conversion of a Lincoln bomber into a flying 'ice wagon' for de-icing research is one of the typical functions of the Napier Flight Development Establishment, undertaken for the Ministry of Supply in the course of the service it provides both for the Ministry and many of the British aircraft and aero-engine manufacturers.

Some Aspects of High Speed Flow

By V. T. FORSTER, B.Sc.(Eng.), A.M.I.Mech.E., Head of the Air Flow Laboratory, Steam Turbine Division.

PART II

Part I of this article was published in the December 1956 *issue of this journal, volume fourteen, number eight, page* 39.

IN THIS SECOND PART of the article some practical applications of high speed flow are examined, and may well be divided into external flows and internal flows. By external flows is meant relative motion between an immersed body and a stream of fluid, e.g., propellers and aircraft. With internal flows the fluid is moving at high speeds relative to some confining shape of duct : examples are nozzles, turbine blades, wind-tunnels, jet pipes and valves. In all such applications the interest is in the changes in the fluid conditions and the interaction of forces taking place between fluid and adjacent solid boundaries.

Early Applications

Until the rapid rise in the speed of aircraft compelled a revision in aerodynamics to allow for the compressibility of the air, interest in fluid motion at high velocities was mainly confined to ballistics and, regarding internal flows, to steam nozzles. It is fairly certain that Admiral Nelson fired his cannon-balls at the French Fleet at speeds exceeding that of sound, but even so, data published on ballistics are few, due no doubt to the association with weapons of war.

The resistance of a body of revolution however, such as a shell, is much lower than that of a two-dimensional wing of the same cross-section, due to the leakage which can take place all round the body, and therefore the critical Mach number is higher. Thus, for a length-to-diameter ratio of 5, the shell has a critical Mach number of 0·9, whilst a corresponding two-dimensional wing with a chord-to-thickness ratio of 5 would have a critical Mach number of about 0·72. The resistance to flow in the transonic region is therefore not so great, and once in the supersonic range there are shock waves at the nose and tail of the body in a similar fashion to those on a wing shown earlier (in Part I), but they are, of course, conical.

Contrary to subsonic flow, it is the forward part of the body which decides the resistance, and the rear can be cut off more or less sharply. This is just as well, as a streamlined shell would cause some embarrassment in the artillery. The effect is shown in Fig. 6, where the comparison is made of the drag of a sphere alone and then with a fairing upstream or downstream or both together. The values of drag co-efficient given apply to a Mach number of 1·5.

A closer look might now be taken at internal flows via the well-known de Laval nozzle, since

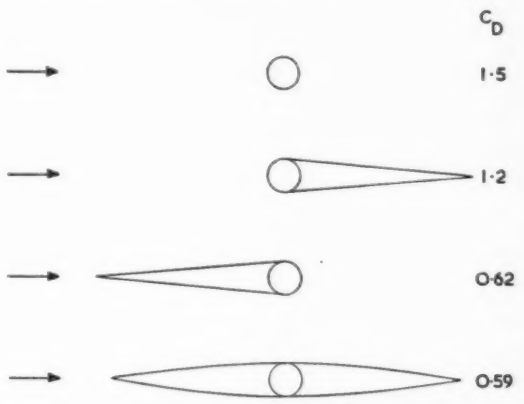

Fig. 6.—*Comparable drag coefficients for sphere and additional fairings at Mach number* 1·5 (*Hoerner*)

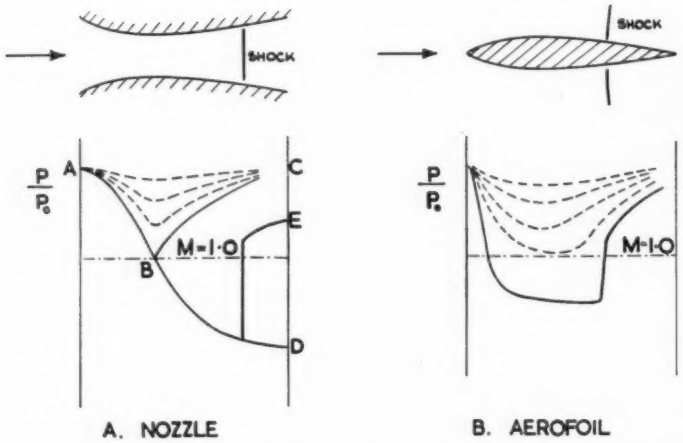

Fig. 7.—Diagrams showing similarity of pressure distribution inside nozzle and around aerofoil

this teaches much about convergent-divergent effects, as well as being of major importance in the design of wind-tunnels, rockets, etc. Fig. 7A shows how the pressure varies through such a nozzle designed for a certain supersonic outlet Mach number and going through sound velocity at the throat. The portion above curve ABC represents subsonic flow, and the curve ABD continued frictionless supersonic expansion down to the specific back pressure. The first important point to note is that whereas in the subsonic region an infinite variety of mass flows and velocities can be accommodated, there is only one shape for the particular supersonic pressure ratio, and one flow quantity fixed by the size of the throat. The question arises, what happens if the pressures are not right for the nozzle shape, or conversely, if the nozzle shape is not right for the pressures.

Suppose that the nozzle operates with an exhaust pressure much higher than that for which it was designed, say at point E. The important point to appreciate is that the pressure cannot just fall smoothly from A to E as might at first be imagined. What it actually does can be determined closely enough by following down the frictionless expansion line ABD and also assuming frictionless subsonic diffusion back from E. There will then be found a position in the nozzle at which the only way the two curves can be joined is by a sudden pressure jump, i.e. a shock wave, usually a normal shock wave. This is an example of shocks occurring inside the nozzle. If the back pressure is below the throat pressure, the shocks will generally occur outside the nozzle, this also applying to pressures below point D.

This necessity for over-expansion of the flow beyond the final outlet pressure is a very significant one, and not only for internal flows, since it also has a bearing in another important application, the pressure distribution on an aerofoil in the transonic range. The similarity of flow conditions can be observed from Fig. 7B, which shows the typical pressure variation on the surface of an aerofoil. Here the subsonic region can again be filled in, to find that on acceleration to supersonic velocities the recompression is again through a shock wave as seen earlier. The effect of this type of pressure distribution on the lifting devices of an aircraft is the problem that has to be faced by the aircraft designer to enable his machine to fly in safety through the sound barrier. The development of the piston-engined aircraft slowed down due to an analogous problem ; it was found that propeller performance was limited as soon as the tip speeds approached that of sound.

Present Problems

Aircraft

It would be impossible in the space available to examine all the problems of an aircraft passing through the sound barrier or transonic region, since so many factors are involved, but limiting the discussion to just the wing, of conventional section and camber suitable for low speed flow, some of the important transonic phenomena can be summarised as follows :—

(1) Somewhere between the critical Mach number and Mach 1·0 there is an extremely steep rise in resistance, i.e. in drag coefficient. From the discussion in Part I this can be explained as being due to the shock stall, i.e. to the increasing intensity of the shock wave development and the tendency

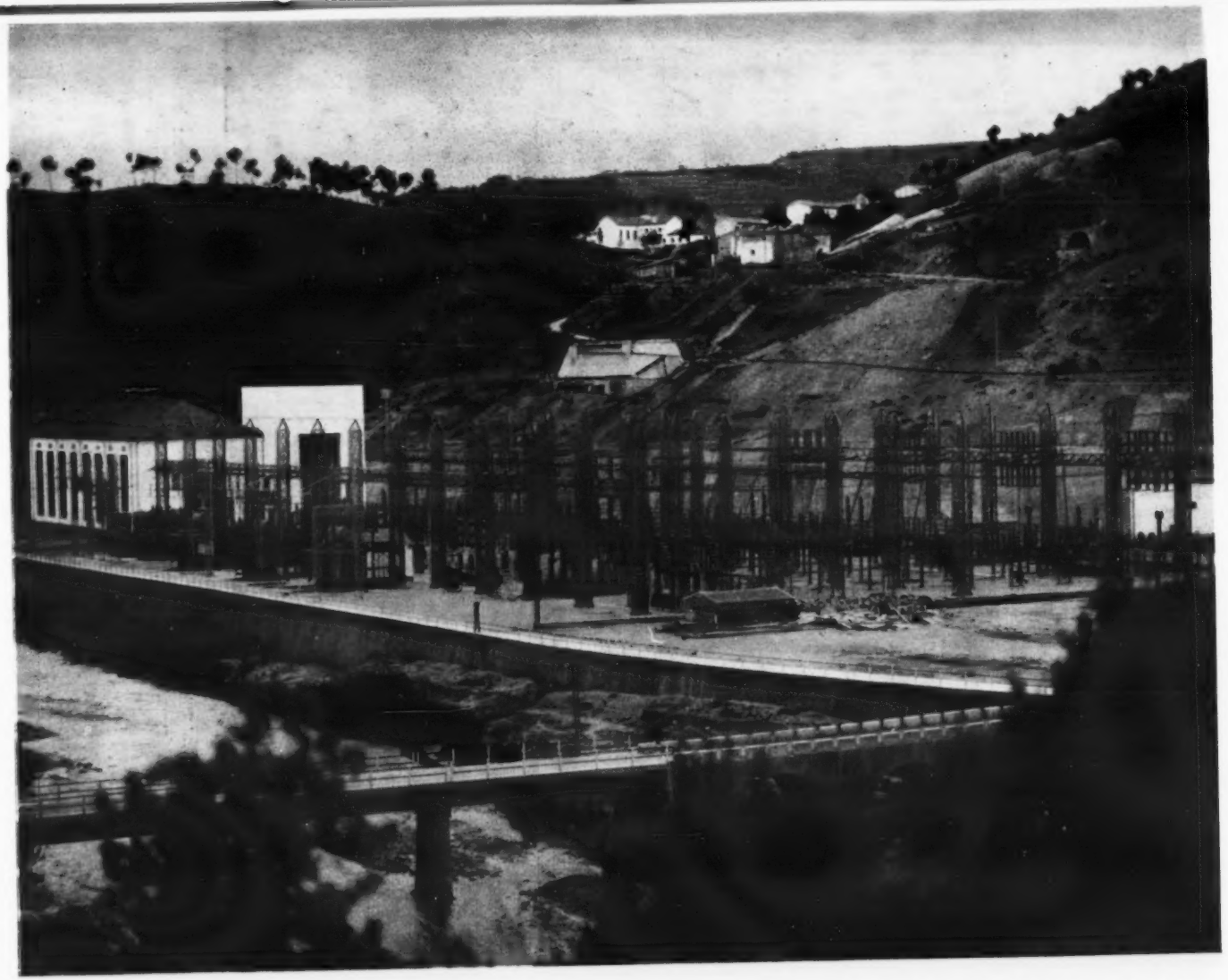

This outdoor switching station, containing twelve 'English Electric' 165 kV 3,500 MVA air-blast circuit-breakers, is at the Cofrentes Power Station in Spain of La Sociedad Anonima Hidro-Electrica Espanola, on the Madrid-Millares 150 kV grid system. The equipment supplied for this power station together with that for Salime Power Station of Saltos del Navia en Comunidad, which is described in the first article of this issue, forms part of The English Electric Company's contribution to the development of Spain's electric power resources

The two centre grabbing cranes in this illustration have recently been installed by Messrs. Stothert & Pitt Ltd., at the Dagenham Dock of Samuel Williams & Sons Ltd., on the north bank of the river Thames to enable rapid unloading of bulk cargoes. Each crane has a rated capacity of 7½ tons for grabbing at 85 ft radius with a total range of lift of 80 ft plus the necessary grab pull-out of 23 ft. The duty cycle specified was twenty-eight seconds for a lift of 30 ft when working from ship to barge, with an alternative cycle of 36 seconds when slewing through 150°.

The electric drives for the hoists of these cranes were supplied by The English Electric Company. To achieve this high speed of operation a special d.c. hoist scheme, employing magnetic amplifiers in the control circuits, was developed since a

conventional a.c. hoist drive was unsuitable for such duty.

The hoist is driven by a d.c. motor of the steelworks auxiliary type, having an armature of low inertia. Its nominal rating is 100 *h.p. at* 485 *r.p.m.* 230 *volts but a speed of* 725 *r.p.m. is achieved with an armature voltage of* 340 *volts. A form of Ward-Leonard control is used in which field forcing is applied to the generator by magnetic amplifiers. Rapid changes can thereby be brought about in the generator voltage and these are translated into rapid acceleration and deceleration of the hoist because of the low inertia of the drive. This hoist scheme is capable of accelerating the grab to speeds of over* 360 *feet per minute in one second. The driver has complete control of the hoist motion through all speeds up to the maximum of* 450 *ft/min.*

The control room in the Fleetwood Power Station of the North West, Merseyside and North Wales Division of the Central Electricity Authority, officially opened on 14*th September,* 1956. *Besides the control room equipment, The English Electric Company supplied the three* 30,000 *kW turbo-alternator sets, the main* 33 *kV metalclad switchgear, the* 3.3 *kV auxiliary switchgear, and the generator, station and unit transformers*

to thickening or breakdown of the boundary layer. As the engine thrust has to overcome the drag, which is proportional to $C_D \times V^2$, unless there is enough in hand it cannot pull the machine through Mach 1·0.

(2) At the same time there is almost as sharp a drop in lift coefficient, on which depends the ability of the aircraft to stay in the air. Whilst the reasons for this are a little more difficult to explain and depend upon the combination of wing section, camber and incidence, it is obvious from Fig. 7A that alarming things can happen since the sum total of the positive pressure on the lower surface and the negative pressure on the upper surface provides the lift force. The rapidity of the fall in lift coefficient, and the exact manner in which it varies again in the transonic region, depend entirely upon the upper and lower shock wave configuration.

(3) In many instances, the reasons for which are uncertain, the shock waves themselves can become unsteady and dance about the wing. This leads to violent fluttering, and the whole aircraft is subjected to what is called buffeting.

(4) The control of the aircraft depends mainly upon the stability of the pitching or longitudinal moment, and thus on the effectiveness of the elevator. The tail-plane/elevator combination will suffer from similar shock-wave effects to those on the wing, and will also in many cases be operating in the slipstream of the main wings. Reaction can, of course, be quite devastating.

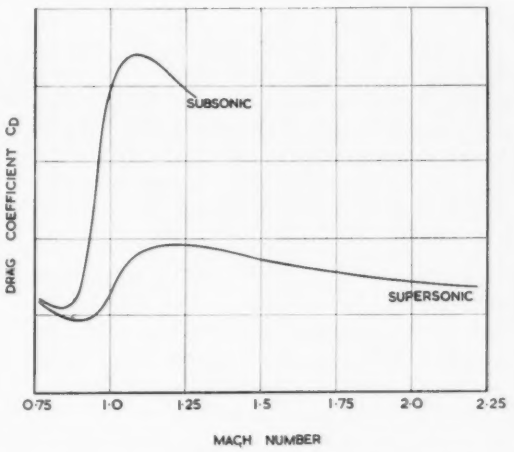

Fig. 9.—Comparison of drag coefficients for subsonic and supersonic fighter designs (Fozard)

The design of aircraft for transonic speeds therefore demands an incessant search for means both of delaying and minimising these shock-wave phenomena. Two of the answers are very much in evidence in the aircraft of to-day, i.e. the reduction in the thickness/chord of the wing, and the introduction of sweepback. Fig. 8 shows the large increase in critical Mach number that is possible using these two devices. Increasing the critical Mach number means, of course, that the intensity of the shock pattern can never grow so much before total supersonic flow is achieved. This is shown in Fig. 9 in which the drag coefficient of a fighter of 10 years ago is compared with that of a supersonic fighter design of to-day.

The idea of sweepback, first put forward by Buseman in 1935, is an extremely simple one, although as might be expected it brings additional

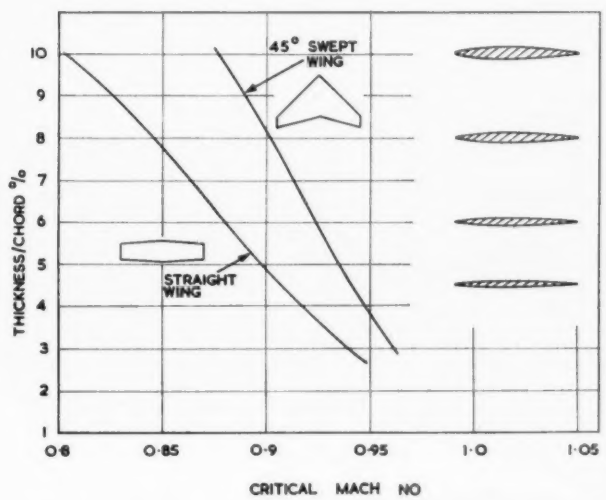

Fig. 8.—Effect on wing critical Mach number of thickness/chord ratio and sweepback (Fozard)

Company supplied the three 30,000 kW turbo-alternator sets, the main 33 kV metalclad switchgear, the 3.3 kV auxiliary switchgear, and the generator, station and unit transformers

problems in its trail. It is based on the fact that the component of velocity which determines the critical Mach number is that normal to the leading edge of the wing. Thus, if the wing is swept back (or forward) by an angle θ, the effective stream Mach number as far as the wing is concerned is M cos θ. Actually the full advantages of the cosine effect are not achieved in practice mainly because of the limited wing span.

Although the foregoing remarks have referred almost entirely to wing performance, it must be remembered that most aircraft consist of a fuselage-wing and tail combination, and as the delay of the shock effects on the wings is continued, the fuselage effects become more prominent. Whilst exhaustive tests have been carried out on aerofoils in two-dimensional flow, the three-dimensional problem of wing and body is not so easy to investigate. The critical Mach number for the combination will be lower, since the air will speed-up round the fuselage and again round the wing. The logical consequence of this is to have both wing and tailplane offset from the thickest portion of the fuselage, and this is another noticeable feature of many of to-day's aircraft.

It is, however, only recently that there was released from the secret list a new and amazingly simple rule for the design of transonic aircraft. It was arrived at after finding a new interference shock wave lying immediately behind and parallel to the wings, and thus not seen on a two-dimensional picture. This area rule, as it is called, states that as far as the shock wave phenomena are concerned, the whole aircraft can be treated as a body of revolution with areas along the axis equal to the total area of the aircraft at any cross-section, this including wings, nascelles, fuel tanks, etc. Having obtained this 'melted-down' body, its shape could then be compared with the optimum, and suitable smoothing carried out. Thus, where the wings join the aircraft the fuselage may have to be pinched in to avoid a sudden increase in cross-section, whilst at the tail it may even be advisable to add some 'metal' in order to fall in with the rule.

Altogether, in spite of increasing knowledge, the transonic region is not a place to linger in, and certainly not to cruise in. The only real answer is to get through it as quickly as possible. Once through, there is a cessation of buffeting, the drag coefficient drops, and the controls begin to behave normally again.

Apart from the mathematical complexities, the reason for delay in acquiring knowledge of transonic flow has been the denial to the aerodynamicist until recently of what had been his most indispensable tool, the wind-tunnel. It is not difficult to generate a Mach number of 1·0 inside the working section of a wind-tunnel, but two difficulties arise when a model is inserted. Firstly, the tunnel immediately chokes because at this Mach number the tunnel is very sensitive to any change in area, as was seen from an earlier equation. Thus the velocity is immediately reduced and tests cannot be made at Mach 1·0 at all. Secondly, unless the model is extremely small compared with the working section area, the nearly normal shock waves developed on the model are reflected back from the walls of the tunnel and impinge on the model again, completely invalidating any readings.

For these two reasons, testing in the transonic range, say Mach number 0·8 to 1·2, was virtually impossible for many years. Several transonic tunnels are now operating however, the problem apparently being solved by the use of perforated or ventilated walls in the working section, which overcome the self-choking restriction and to some extent the shock wave interference effects.

Supersonic tunnels are actually more commonplace than transonic tunnels, though the size of working cross-section is usually limited by power requirements. The acceleration to supersonic speeds has to be obtained in a curved expanding nozzle very carefully designed so that a uniform Mach number is obtained. One-dimensional flow equations are altogether too crude, and the method of characteristics already mentioned is usually employed. Even then, however, if a change of Mach number is required, a completely new nozzle shape is called for ; in many tunnels this is done by using flexible walls for the nozzles.

Aerofoils in Cascade : Turbo-machines

Having just examined some of the problems involved as the speed of aircraft is increased through the transonic range, it must be remembered that in jet machines the air has to go through the

aircraft as well as round it, and this introduces three further problems ; first to get it into the aircraft, then to pass it through the engine and then to eject it, and all these become more acute as the forward speed increases. The intake and exhaust will be discussed later, in order first to mention the turbo-compressor unit and study how increased velocities affect this.

All types of axial-flow turbo-machines are in essence made up of rows of aerofoils in which deflection of the fluid and changes in velocity and pressure take place. Several factors complicate the examination of high speed flow through such cascades of blades, as they are sometimes called : (1) the mutual interference of the blades, (2) the pressure before and after the row is nearly always different, (3) the fluid is changed in direction as it passes between the blades, (4) if the flow through the cascade becomes anywhere supersonic, the velocity and pressure at outlet cannot become uniform as with a subsonic design, (5) there is an infinite variety of blade shapes.

However, it is possible to generalise to some extent, and an attempt is made in Fig. 10 to give an introductory if over-simplified picture, using as a link with aircraft a cascade of aerofoils of zero camber.

For the examples shown, the mass flow through the cascade can be continually increased until at some point a local shock wave will begin to form. In case (B) a certain approach Mach number will be reached when a shock wave, with its attendant phenomena, develops near the narrowest section. Obviously, the closer the pitching and the thicker the aerofoils the lower will be the critical Mach number. For the accelerating cascade of case (C), the highest velocities are at the outlet, and it is here, and usually on the convex surface, that a shock wave first appears. Since this shock cannot upset the flow through the passage, it might be assumed that in the transonic range Mach number effects on this type of blade are not very marked, and this has been amply proved by the large amount of experimental work done on nozzles using both steam and air. In the decelerating cascade of case (D), however, widely used in axial flow compressors, the maximum velocities are at inlet, and the first shock wave occurs on the convex surface near the point of maximum suction. The immediate tendency is to separate the flow in this region, and if this happens the performance of the whole passage is jeopardised. It is thus found that this type of compressor blade is limited to an inlet Mach number of 0·7 to 0·75, although serious attempts are being made to increase this by the use of sharper leading edges, and by moving back the position of maximum thickness.

Case (E) is the intermediate example of an impulse type blade where there is a large deflection but little pressure change. Here the likelihood is that the velocity will first reach that of sound near the middle of the passage and on the convex face, there being a velocity gradient across the passage due to centrifugal effects.

It should be noted that in all these examples except (A) there will be a limiting inlet Mach number which cannot be increased since the blades

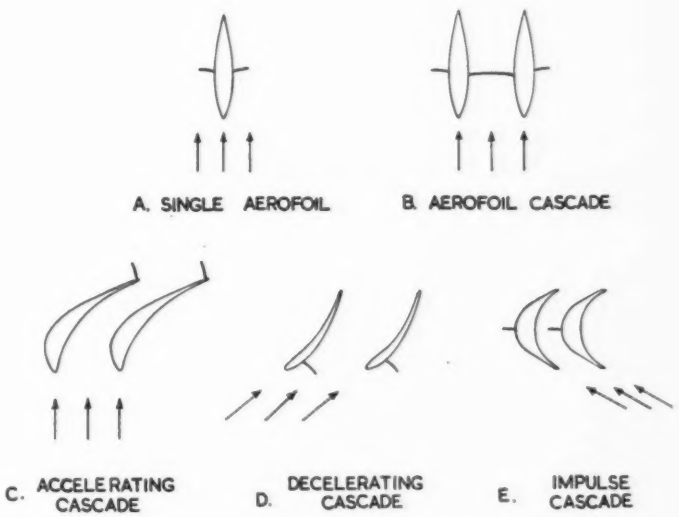

Fig. 10.—Diagrams showing first formation of shock waves on typical blade cascades

will be choked, i.e., Mach 1·0 will be reached at some throat.

The design of aircraft engines for high working Mach numbers presents therefore a complex picture, but it is obviously desirable as the consequence would be a reduction in both size and weight.

Turning now to steam turbines, which have in fact been running at transonic Mach numbers for some time, rather curiously the two places in the turbine where high Mach numbers most often occur are at the beginning and the end. In the high pressure cylinder the designer often likes to take out a large heat drop across a single or two-row Curtis stage, this stage being an important component on single cylinder machines, particularly for marine work. At the low pressure end of large condensing machines enormous volumes of steam are exhausted, and in order to keep down both the length of the last row and the size of the exhaust branch the designer is forced to use high steam velocities. The velocity of sound in steam at 28½-29 in vacuum is around 1,230 ft/sec, so that the velocities are often increased to Mach 1·0 and over in the last stage.

It might be asked how all the various shock wave phenomena that have been discussed are affected if the working fluid is not air but steam. Although little experimental evidence is available, the likelihood is that the differences are small, since, if the Mach numbers are the same, the only other factor that matters is the adiabatic index γ, which is respectively 1·4, 1·3 and 1·135 for air, superheated steam and wet steam. Fig. 11 shows sets of curves corresponding to three of the most important formulae in high speed flows which might be expected to introduce discrepancies.

The first set of curves shows the important isentropic relationship between pressure ratio and Mach number, the second shows how the deflection of the stream varies, which is very important in any supersonic expansion, and the third the variation of Mach number across a normal shock wave. Thus, if limited to a maximum Mach number of about 1·5, the differences are only of a small order.

In verification of this, Fig. 12 shows comparable shock wave pictures of the same reaction blade using both air and superheated steam, at a Mach number of around 1·26. The simple optical techniques already mentioned were used for both, and as can be observed, the shock pattern is very similar.

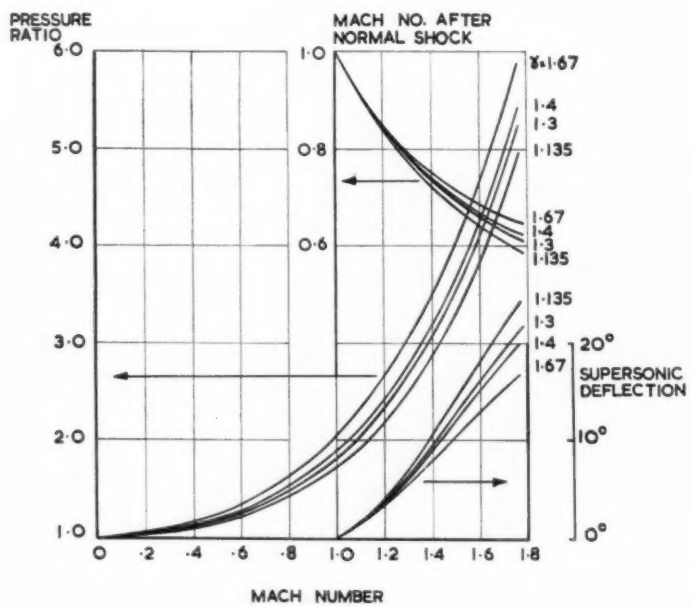

Fig. 11.—Curves showing influence of adiabatic index γ on some important Mach number relationships

Flow in the L.P. cylinder is further complicated by wetness and by very low Reynolds numbers, so that the combination is that of shock waves, viscous flow, and water particles—rather an unpredictable mixture.

Returning to the Curtis stage, the large heat drops involved often result in Mach numbers of 2·0 or higher out of the first nozzle row, and the nozzles have to be shaped convergent-divergent in order that the supersonic speeds may be efficiently achieved. However, they are only right for one Mach number, as can now

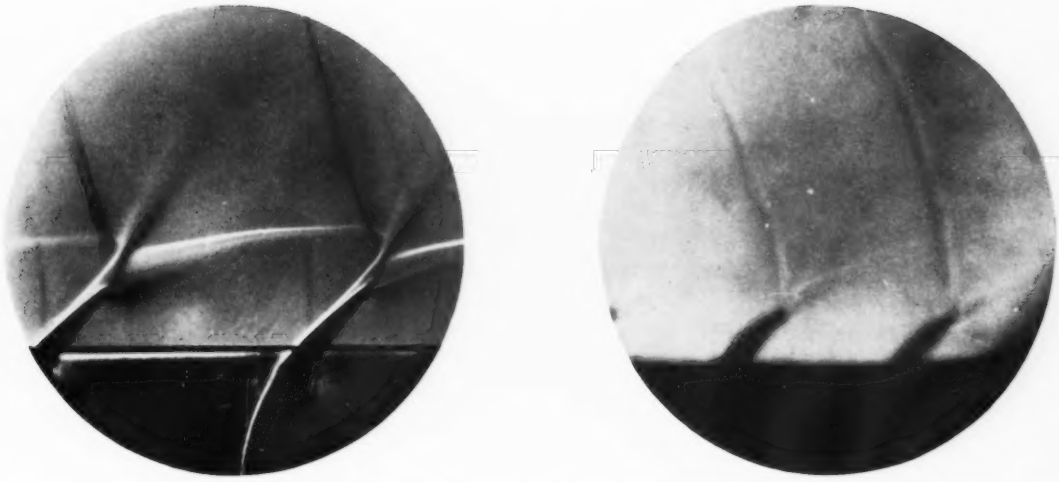

Fig. 12.—*Reaction blade shock wave pictures using both air and steam. Left* : *Air, Mach number* 1·26 (*Schieren photograph*). *Right* : *Dry steam, Mach number* 1·30 (*Shadow photograph*)

be appreciated, so that a change in load or speed will introduce shock waves and extra losses. This can be overcome if the Mach number is not greater than about 1·4 by using a simple convergent nozzle, the fluid creating its own divergence beyond the nozzle throat. This is probably because the shock waves formed do not jeopardise the passage flow, and the shock losses themselves are not appreciable until beyond this Mach number. This has been proved by measuring the total head variation with a traversing pitot tube at the outlet of a typical turbine nozzle shown in Fig. 13. This picture was obtained using air, and the outlet Mach number is 1·28. It was found that the only losses were those in the wake until a Mach number of about 1·2 was reached ; beyond this there was an increasing loss measured in the flow from the passage, which could only have been due to the presence of the shock waves themselves.

Space permits only brief indication of a few other applications where Mach number effects are involved. Blast waves are an obvious example, both in air and under water, and there are the transient wave phenomena in internal combustion engine exhaust systems; these and other analogous problems involving reflection, refraction and collision of shock waves are being studied by means of the shock tube. There are the flame fronts met in combustion work with the added complication of change in chemical energy across the shock. In

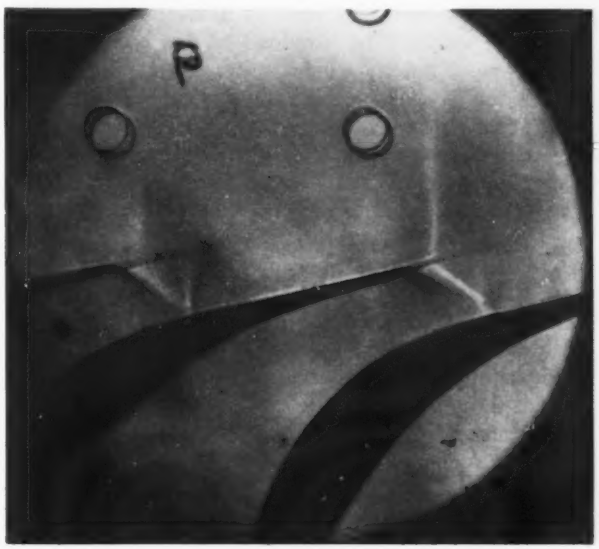

Fig. 13.—*Flow through steam turbine nozzles using air at a Mach number of* 1·28 (*Schieren photograph*)

the electrical sphere air-blast circuit-breakers may be mentioned.

Future Possibilities

To conclude this article a reference is now made to one or two aspects of entirely supersonic flows.

Aircraft

The sound barrier itself has almost been breached, and we shall soon be in the clearer field of aircraft cruising at supersonic speeds, with quite a long way to go before the slope of the thermal barrier becomes too steep. Specialised aircraft are already well on the way, and with such increase in speeds the internal shape of the aircraft will present more problems than the external shape. This is because fairly straightforward theories have been evolved for the latter, which enable the characteristics of slender wing-body combination to be predicted reasonably closely. As the Mach number increases, however, a larger percentage of the pressure required for combustion is achieved at the aircraft intake due to the ram effect, and at supersonic forward speeds this has to be done, of course, through shock waves. The efficiency with which the pressure recovery is utilised and its matching with the turbo-compressor unit therefore play a big part in the final value of aircraft thrust. The pitot type of intake, such as is used in the 'English Electric' P-1A, swallows its air requirements through a normal shock wave. This is the least efficient type of shock but is satisfactory up to Mach numbers of about 1·5. Beyond this the pressure rise is accomplished much more efficiently through a series of inclined shocks. Such a shock pattern necessitates a pointed central body from which the first inclined shock can spring, and preferably the body should be adjustable so that the variation, required with speed, of both shock angle and area can be accommodated.

Similar considerations are pertinent to the other end of the aircraft, i.e. the exhaust nozzle. At low supersonic Mach numbers it is satisfactory to use a simple convergent nozzle, just as in the turbine. At higher Mach numbers a convergent-divergent shape will be necessary in order to expand efficiently down to atmospheric conditions. Once again, however, some method of altering the throat to exhaust area will be required for efficient operation over a wide range of Mach numbers.

Going higher still, beyond Mach 2·0, all the pressure rise required can be obtained at the intake, which means that the compressor is superfluous. For example, a Mach number of 1·6 or so is sufficient to give a 4 : 1 pressure ratio (see Fig. 11). Further, since the turbine is only there to drive the compressor, this can also be omitted, and the simple ram-jet is arrived at with no moving parts ; just an intake, combustion chamber and exhaust.

Turbines and Compressors

On present conventional turbines and compressors, supersonic velocities are reached at the few isolated points already mentioned and also at the tips of centrifugal compressors, but probably the only blades which might be immersed in a completely supersonic stream are those making up the first moving row of a high pressure ratio Curtis stage. The words 'might be' are used advisedly since although the velocity diagrams can be drawn down in the usual manner from the available heat drops, which suggest supersonic velocities at inlet and outlet, it is difficult to see, bearing in mind the latest knowledge of high speed flows, how such supersonic

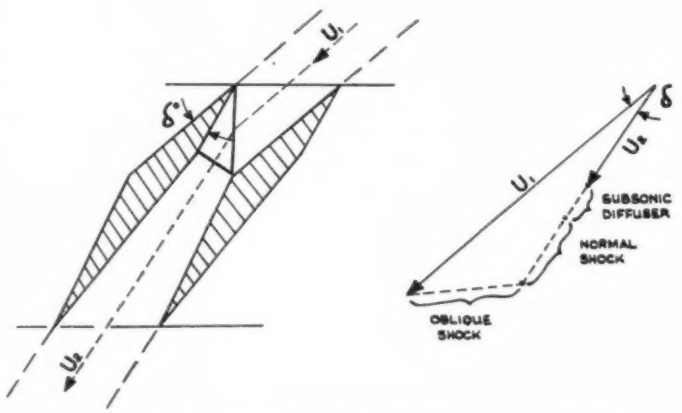

Fig. 14.—Possible supersonic blade for axial flow compressor, with corresponding velocity diagram (Schnell)

velocities can in fact exist without most careful geometric detail. The problem is so to design the passage and incident flow that breakdown of the supersonic stream is avoided, and then to deflect the fluid through the required angle without intense shock formation.

The supersonic engine for aircraft, where high throughputs are essential, does not seem to have arrived yet however, although Davidson in 1947, Loeb in 1949 and Schnell in 1955 have reviewed the possibilities of the supersonic compressor, with the reminder that a shock wave is in fact a most efficient diffuser taking up no space, and all that remains is to harness this natural gift to a practical machine. Davidson mentions two single-stage compressors which had actually been built, but neither had been successful although mainly for mechanical reasons.

Much research however is proceeding, and there is good reason to believe that engines in which the first compressor stages are partially supersonic are already nearing the flight stage. It is interesting to note that the blade geometry details and velocity triangles are quite straightforward, assuming no boundary layer complications, and Fig. 14 shows a possible blade row for either rotor or stator. In this example the blade is designed for a particular supersonic inlet Mach number and incidence such that an oblique shock followed by a normal shock are produced, with subsonic diffusion thereafter to the trailing edge ; the equivalent velocity diagram is also given.

One of the major problems obviously is that encountered in all supersonic flows, the fixed geometry suiting only one fixed set of fluid conditions. Any slight change in quantity or speed is likely to break down such a finely balanced system, and the question arises as to what happens at off-design conditions, and in fact how the machine would run up to speed ; also what would be the surge characteristics of such a compressor ?

Nevertheless, provided the Mach numbers are kept below about 1·5 there are no doubt possibilities for such a machine, and the author feels that if the powerful aerodynamic tools available are applied to the problem of supersonic flows in rotating machinery, vital progress will be made.

BIBLIOGRAPHY

HOERNER, S. F. *Aerodynamic drag*. The Ottobein Press (1951).

FOZARD, J. W. *The supersonic fighter*. Flight (December 10th, 17th and 24th, 1954).

DAVIDSON, I. M. *Some data pertaining to the supersonic axial flow compressor*. R. and M. No. 2554 (May, 1947).

LOEB, W. A. *A study of the supersonic axial flow compressor*. Journal of Applied Mechanics (March, 1949).

SCHNELL, E. *Problems of supersonic axial compressors*. Engineers Digest (August, 1955).

The Applications of Analogue Computors in the Development of Guided Weapons

By R. W. WILLIAMS, B.Sc., Ph.D., A.Inst.P., Guided Weapons Division.

THE IDEA OF DETERMINING the properties of one physical system by substituting for it another, possessing the same (or very similar) formal representation of its behaviour but which is more amenable to observation and calculation than the first system, is well established and is of particular value in the field of guided weapon development. In this field, the manufacture of test vehicles and the conduct of their subsequent flight trials is an extremely expensive undertaking, and the use of analogue computors and simulators to facilitate the study of the system for which they stand proxy, prior to these trials, has become a prominent feature of the guided weapons industry.

It is a matter of common knowledge that there are two main classes of computing device—analogue and digital. In the former, physical quantities such as voltages or the angles of rotation of shafts, are used to represent the variables on a proportional basis, whereas in the latter, numbers are handled in digital form and the ultimate function which is performed is that of counting. Analogue methods cannot compete with those of digital computing in matters of accuracy, but paradoxically digital computors, in spite of the high speed at which the basic operations are performed, are as yet not fast enough to handle large system problems in real time (that is, the solution time in the computor is required to be the same as the elapsed time in the system being studied), and the field of application of analogue computors is assured for a long time to come.

In their application to guided weapon problems, analogue computors offer the following major advantages :—

(i) In such fields as trajectory computation and assessment work they enable data to be amassed quickly and easily, with sufficient accuracy for the purpose in hand. The effects of varying the parameters of the system are rapidly ascertainable, and the most fruitful areas for exploration are readily revealed to the designer.

(ii) Actual components of the weapon system may be incorporated in a computor. For example, in studying the properties of a missile control system, an analogue computor might be used to solve the equation of motion of the airframe, a set of control-surface actuators being connected in to the computor so as to receive the appropriate input signals, and in turn feed back to the computor voltages representing the control-surface deflections. The analogue technique from its very nature is well able to meet the requirements for marrying computing facilities and system components. The use of components in this manner contributes a great deal to the realism of the simulation. It may be noted that the terms ' analogue computor ' and ' simulator ' are practically synonymous ; the term ' simulator ' often implies the incorporation of components in the computing set-up.

(iii) Computors and simulators are invaluable in conveying to the designer the physical ' feel ' of the system and bringing home to him a sound concept of its functioning, since he must know exactly what he is simulating before setting up his simulator facilities.

In many of the problems handled by analogue computors, current time is the independent variable t, and the problems are tantamount to the solution of sets of simultaneous differential equations in t. There is, however, an important application of analogue methods to the solution of algebraic equations, and several computors for

solving sets of simultaneous linear equations, and others—known as isographs—for solving polynomial equations, have been described in the literature. An isograph for the solution of equations of the sixth degree has been in service in this Division for some years. Mention must also be made of computors in which resistance networks are set up and used to solve partial differential equations. When time is the independent variable in the equations, there is no restriction to computing in real time (except when system components are included) and it is very often convenient to set up a computor so that it computes in a machine time t' related to the real time of the original problem by the equation $t' = \lambda t$ where λ is a suitably chosen constant. If λ is much smaller than unity, the computor may then be operated on a repetitive basis, that is, the solution is repeated say 50 times per second and a cathode-ray tube display is made of it which is presented to the operator on a quasi-stationary basis. This technique is specially valuable in studying the response of a system to a step function input signal.

As regards the engineering methods which are required to realise the operations of analogue computing, electronic and electro-mechanical devices are the most frequently employed, since these techniques are the most flexible and have been fully developed for other purposes. Throughout the analogue computing field there is very great emphasis on the use of servo-mechanisms and negative feedback, as will be made clear by examples. Analogue computors may be classified as either special purpose or general purpose ; these descriptions are practically self-explanatory, but it may be added that ' general purpose ' usually refers to a machine of the differential analyser type, which is able to solve a wide variety of differential equations and which comprises a collection of basic units (summing units, multipliers, integrators, etc.) interconnected according to the requirements of the problem in hand. Machines of this type, employing the electronic technique, are in use in the Guided Weapons Division, but the examples which follow are of special purpose computors.

Analogue computors are however also being used in The English Electric Company's Aircraft Division and principal Works, and general purpose analogue computors have been employed in the Nelson Research Laboratories of the Company since 1949.

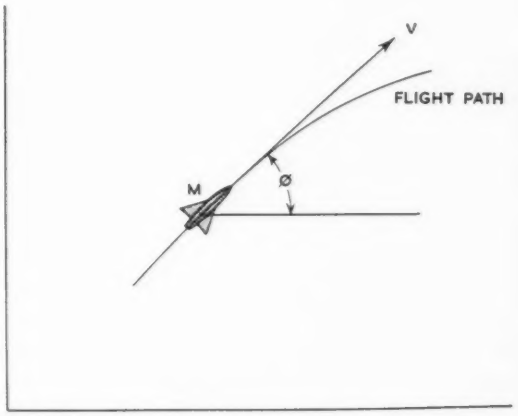

Fig. 1.—Geometry of missile trajectory

Trajectory Computation

Nature of the Problem

A trajectory computor has been in continuous service in the Division since the end of 1951, and it may be cited as a fair example of a special purpose computor whose construction has been justified economically by the volume of work which it has handled. It does nothing that could not be done by the methods of numerical analysis, but it produces results, of an acceptable standard of accuracy, far more quickly than could a human computor using these methods with the assistance of a desk calculator. The nature of the problem solved by the computor may be understood by reference to Fig. 1, which shows a missile of mass M flying with velocity V in a vertical plane. If the tangent to its flight path makes an angle ϕ with the horizontal, then immediately, for free (i.e. ballistic) flight :—

$$M(\dot{V} + g \sin \phi) = P - D_0 \ldots\ldots \quad (1)$$

$$V\dot{\phi} + g \cos \phi = O \ldots\ldots\ldots\ldots \quad (2)$$

Here P denotes the thrust of the rocket motor, and D_0 is the aerodynamic drag on the missile.

In free flight, the missile does not develop any incidence. If however the missile is caused to follow a particular path by the operation of its control surfaces—for example, climb at a constant

value of ϕ, homing flight or programmed flight—incidence is developed and equation (1) must be replaced by :—

$$M(\dot{V} + g \sin \phi) = P - D_0 - D_1 \ldots \quad (3)$$

Here D_1 is the induced drag brought into being by the incidence. Also instead of equation (2), it must be written : ϕ = a function whose nature depends on the navigational demands on the missile. In the simplest cases it might be that ϕ = constant, or $\dot{\phi}$ = constant, etc.

Having stated the basic equations, the terms in them must now be considered in greater detail. The mass M will vary with time since the rocket motor consumes fuel during the flight. In the simplest case a constant rate of burning $(\dot{M})_1$ may be assumed, so that :—

$$M = M_0 - (\dot{M})_1 t \ldots\ldots\ldots\ldots\ldots \quad (4)$$

where M_0 is the initial value of the mass, at $t = o$. Alternatively it may be more realistic to assume a constant $\ddot{M}$, in which case M is a quadratic function of t. The thrust P is quite simply related to $\dot{M}$; it is in fact $\dot{M}\, I$ where I is the specific impulse of the rocket motor. To allow for the slight variation of thrust with altitude, a height function $f_1(h)$ may be included so that finally :—

$$P = \dot{M} I f_1(h) \ldots\ldots\ldots\ldots\ldots\ldots \quad (5)$$

Usually $f_1(h)$ is not greatly different from unity.

Turning now to the drag terms, D_0 for supersonic flight may be expressed quite simply in terms of two main parameters A_2 and B_2 :—

$$D_0 = \psi (h) \left(A_2 \frac{a}{a_0} + B_2 V\right) \ldots\ldots\ldots \quad (6)$$

Here a/a_0 is the sonic speed ratio, and $\psi(h)$ is another height function, $a/a_0 \cdot \rho/\rho_0 \cdot f_2 (h)$, where ρ/ρ_0 is the air density ratio and f_2 is linear, differing very little from unity. The values of A_2 and B_2 will of course depend on the size and configuration of the missile.

The operation of the computor is restricted to the supersonic regime so that the expression for D_0 applies at all times. The induced drag D_1 is expressible as:—

$$\frac{n^2(Mg)^2}{(A_3 V + B_3)\, a/a_0\ \rho/\rho_0} \ldots\ldots\ldots\ldots \quad (7)$$

where A_3, B_3 are parameters and n is the total lateral acceleration experienced by the missile. So far it has been implied that the motion of the missile is confined to a fixed vertical plane, and only one angle, ϕ, has been necessary to specify the direction of the tangent to its flight path. In the general case of three-dimensional motion the vertical plane can be regarded as no longer fixed but continuously altering in its orientation relative to a fixed datum plane, the angle between the planes being an azimuth angle θ. The equation for n is then :—

$$(ng)^2 = (V\dot{\phi} + g \cos \phi)^2 + (V \dot{\theta} \cos \phi)^2 \ldots \quad (8)$$

Note that in free flight, $(V\dot{\phi} + g \cos \phi)$ and $\dot{\theta}$ are each zero so that D_1 is zero, as already stated. In forced flight, θ, like ϕ, is some function whose nature depends on the navigational demands on the missile.

The basic equations have now been stated. To complete the formulation of the thrust and drag terms, the height h must be known and this is obtained by integration of the vertical component of V: $h = \int V \sin\phi dt$. Similarly, the position of the missile as regards northings and eastings displacements from a datum point is found from $\int V \cos\phi \cos\theta dt$ and $\int V \cos\phi \sin\theta dt$.

Computing Technique

The electro-mechanical technique is employed throughout the machine, the analogues used being 50 c/s voltages and shaft rotations. The principal computing units are 11 integrators (which embody a 50 c/s version of the well-known Velodyne principle) and 3 position servos together with their associated servo amplifiers, summing—and buffer—amplifiers, etc. Multiplication is effected by means of potentiometers installed in the integrators and the position servos ; the functions of height are generated by means of potentiometers, and Magslip feedback resolvers yield the trigonometrical functions. The integrators are scaled so that the machine operates on a 1 : 1 time scale. The mechanical units and their associated electronic units are rack-mounted on a plug-in basis for ease of maintenance. Fig. 2 gives a general view of the computor, and Fig. 3 shows the associated plotter (this is the height plotter of an anti-aircraft predictor modified to suit the Division's requirements) which records the computed trajectories.

Fig. 3.—Plotter for trajectory computor

Almost all the trajectories handled by the machine are smooth curves, with modest time rates of change of the variables. In consequence, the dynamic performance of the servos is not called seriously into question and the choice of such a low carrier frequency as 50 c/s is not disadvantageous. Space does not permit a full account of the block diagram of the computor to be given, but the evaluation of the important quantities ϕ and V will be described to illustrate the technique. In Fig. 4, the servo amplifier A feeds the controlling phase of the 2 in. Magslip 50 c/s 2-phase induction motor M, which is coupled mechanically to the 2 in. Magslip induction generator G. The output of G, after buffering, is multiplied by V by means of the potentiometer shown, and the switch S_2 offers the choice of either $V\dot{\phi}$ or $\dot{\phi}$ as the feedback signal. The input signal to the servo is selected by S_1 to be either a navigational or programmed demand for $\dot{\phi}$ (or $V\dot{\phi}$), or the term $-g \cos \phi$. This latter is obtained from the Magslip feedback resolver MR1 whose rotor is gear-driven from M.

Fig. 2.—Trajectory computor

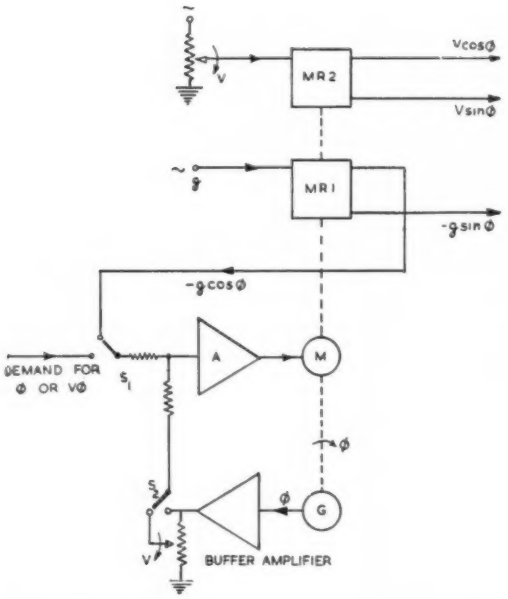

Fig. 4.—Computation of angle of elevation, ϕ

The input signal to MR1 is a constant 50 c/s voltage representing g. For free flight, the switches are set so that the net signal to the input grid of the servo amplifier is $-g\cos\phi - V\dot{\phi}$, and the servo functions to hold this at very nearly zero. Similarly for forced flight, the servo runs so as to provide a feedback signal which balances the input demand fed in through S_1. The switches are in fact relays, which are controlled from a central position so as to give a change-over, if necessary, from free flight to forced flight or *vice versa*, in mid-trajectory.

The second resolver installed in the ϕ unit is fed with a signal from a V-driven potentiometer, so as to yield output signals $V\cos\phi$, $V\sin\phi$, which are required elsewhere in the computor.

Fig. 5 illustrates the computation of V, based on equation (3), and which is produced as a shaft rotation. Three summing arms are used as shown to deliver signals representing $-P$, D_0 and D_1 respectively to the input grid of the V servo amplifier. The induction generator output, $-\dot{V}$, is buffered and then combined with $-g\sin\phi$ (already available from the ϕ unit) in the summing amplifier shown. The output of the latter is multiplied by M by means of a potentiometer installed in the mass integrator so as to yield the final feedback signal $M(\dot{V}+g\sin\phi)$ which balances the input signals. Those inputs are now considered in a little more detail. A potentiometer driven for $\dot{M}$ is the starting point for the thrust term. It feeds directly a graded potentiometer, driven for h, which introduces $f_1(h)$. Finally the specific impulse is introduced by making part of the P input arm a potentiometer used as a variable resistance. This potentiometer is provided with a dial calibrated to read directly in I. The computation of D_0 is straightforward. A potentiometer driven for h gives a/a_0 as a start ; this feeds a potentiometer driven for A_2. The term B_2V is produced by means of cascaded potentiometers as shown. A summing amplifier yields $A_2a/a_0 + B_2V$ and there is a final multiplication by ψ (h) in a graded potentiometer. The computation of D_1 is

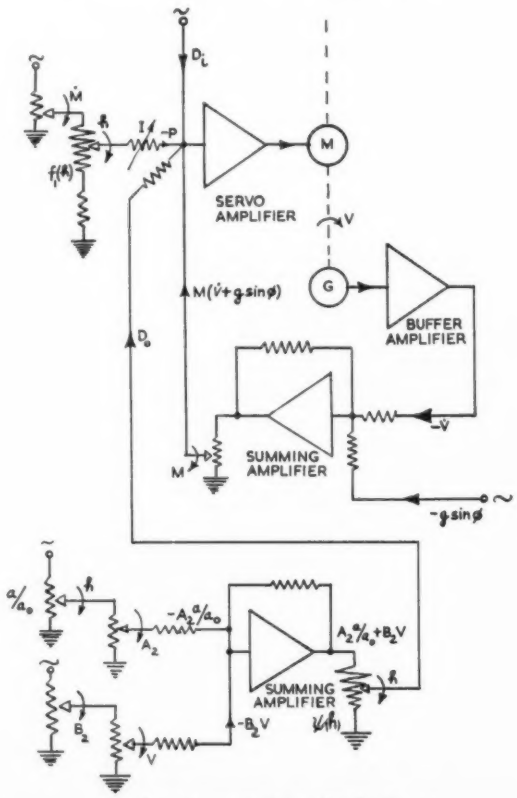

Fig. 5.—Computation of velocity, V

based on equations (7) and (8) and will not be described. The remaining operations performed in the computor are summarised below :—

(i) A double integration of $\ddot{M}$ to yield first M and then M itself. The burning characteristics of the rocket motor can be quite accurately represented by selecting an initial value of $\dot{M}$ and a constant (or very simply programmed) value of $\ddot{M}$.

(ii) Resolution of the horizontal component of V into northing and easting components.

(iii) Integration of the velocity component to yield co-ordinates of missile position, in particular the height, which must be known for the computation of the various aerodynamic functions of height.

(iv) Computation of the navigational demands for $\dot{\theta}$ and $\dot{\phi}$.

Exactly the same techniques as have already been described are used for all these operations.

Accuracy Attainable

The following figures for computing accuracy may be quoted for the various units in the computor, all figures being expressed on a '% of full scale' basis and referring primarily to steady-state conditions :—

Integrators	±0·3%
Function generation :	
Resolvers	±0·1%
Potentiometers, best case..	±0·1%
Potentiometers, worst case	±1·0%

It is difficult to specify the overall accuracy which is achieved, but it is worth stating that the users suspect the performance of the machine if a standard test trajectory is tried and V is observed to have values which differ by more than about ±30 f/s from the numerically-computed values. Similarly, the height is computed to within a few hundred feet of the truth. Repeatability of results is generally to much closer limits than those quoted for the overall accuracy. In general, it is the Division's experience that the trajectories evaluated by the computor form an adequate basis for predicting the trajectories of test vehicles in flight.

Missile Response Simulation

As an example of the use of analogue computation in association with missile components, a missile response simulator is now described which has been employed extensively for the investigation of control system performance.

Consider the right-handed system of axes x, y, z, which coincide with the roll, pitch and yaw axes of a missile. The components of the missile velocity vector along these axes are u, v, w ; the missile spin vector has components along the same axes p, q, r. If the rudder and elevator angles are ξ and η, the equations of the missile motion may be written as :—

$$\dot{v} = \xi y_\xi + v y_v + g_y - ru + pw \quad \ldots\ldots \quad (9)$$

$$\dot{r} = \xi n_\xi + v n_v - (1 - A/C)\, pq \quad \ldots\ldots \quad (10)$$

$$\dot{w} = \eta z_\eta + w z_w + g_z - pv + qu \quad \ldots\ldots \quad (11)$$

$$\dot{q} = \eta m_\eta + w m_w + (1 - A/C)\, pr \quad \ldots\ldots \quad (12)$$

In these equations, y_ξ, y_v, n_ξ, n_v, z_η z_w, m_η and m_w are the aerodynamic derivatives, g_y and g_z are components of the acceleration of gravity, A is the moment of inertia of the missile about the x axis, and C is the moment about the z axis (assumed to be the same as that about the y axis). In the computor which is set up to solve equations (9)-(12), various simplifying assumptions are made, notably that the aerodynamic derivatives are constant, as are also p and u. As a consequence of these assumptions, the aerodynamic derivatives and the quantities p and u are fed into the computor as hand settings of potentiometer dials, so that when the missile is 'flown' at different heights and forward speeds and for different values of the rate of roll, p, the operator alters these settings from run to run, to allow for the dependence of the derivatives on height and speed. The adoption of the assumptions greatly simplifies the design of the computor, since the need to provide electronic multiplying units to evaluate such terms as ru, pw, etc., is obviated.

In the missile itself, the input signal to a rudder or elevator servo is the difference between a navigational demand and a feedback signal which is the output of the yaw or pitch rate gyro suitably processed. In the simulator, the navigational demand is replaced by an input signal chosen by

the operator to suit his purpose, for example, a step or ramp function or a steady sinusoidal oscillation of adjustable amplitude and frequency. The rate gyro output is replaced by a voltage representing q or r which is available from the computor. The relationship between the computor and the missile control-surface servos will be made clear by perusal of Fig. 6, which is a schematic diagram of the rudder channel of the simulator (the elevator channel is identical in form). The computor portion of this comprises four high-gain d.c. amplifiers, two of which are provided with capacitative feedback so that they function as integrators, the remaining two having resistive feedback so that they act as sign-reversing units, having unity overall gain. The integrators are fed with input voltages representing the individual terms which are to be found on the right-hand sides of equations (9) and (10), and their outputs are therefore representative of $-v$ and r respectively (the negative sign of v is a matter of convenience and has no special significance). Note how potentiometers, hand set for the various derivatives, are used to form the input signals to the integrators. In the case of the ξn_ξ and ξy_ξ terms, the excitation for their potentiometers is derived from a potentiometer coupled to the output shaft of the rudder servo, and whose slider is therefore driven for ξ. The exciting voltages for the remaining potentiometers are all available ; v, $-v$ and $-r$ from the outputs of the computing amplifiers in the rudder channel itself, q, $-q$, w and $-w$ from the computing amplifiers in the elevator channel. The components of the acceleration of gravity, g_y and g_z, are available only if the missile attitude angles in a fixed frame of reference are being evaluated in a separate computor ; with the simulator used only for control loop studies, g_y and g_z are omitted.

Having seen how a signal representing the yaw rate gyro output is produced, the formation of the input signal to the rudder servo is now considered. The gyro output is processed in the missile by the

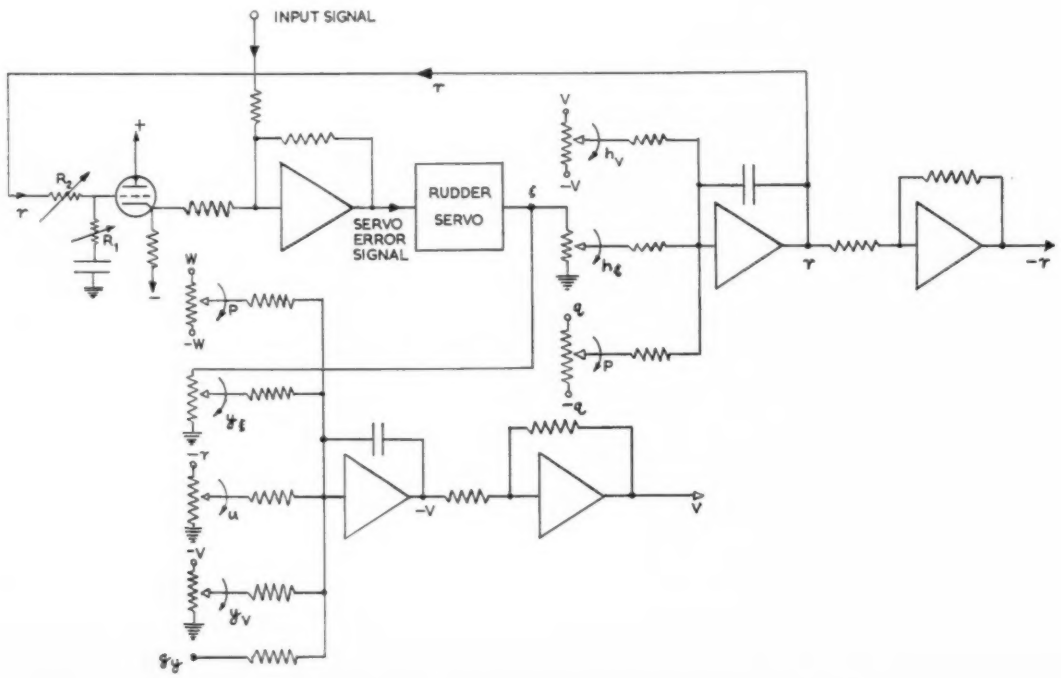

Fig. 6.—Schematic diagram of rudder channel, missile response simulator

transfer function $\frac{1+T_1 s}{1+(T_1+T_2)s}$, where s is the Laplacian operator. This transfer function is realised by the passive network which appears at the left-hand side of Fig. 6, the time constants being adjustable by alteration of the resistance arms R_1, R_2, as shown. A cathode follower stage buffers the output of the network, and a summing amplifier (i.e. a high gain d.c. amplifier with resistive feedback) is used to combine the input demand signal with the follower output, thus forming the input signal to the rudder servo.

The association of computor and control-surface servo in the manner described has proved to be of considerable value ; although a servo system may function adequately when tested by itself, unsuspected deficiencies in its performance may well be revealed when an external loop is closed round it, as is done in the present example. Several refinements have been added recently to the simulator which have further enhanced its usefulness ; these include the incorporation of the effects of control-surface incidence—and lateral acceleration—limiting, simulation of the transfer functions of the rate gyros and of the body bending modes of the airframe.

Since the number of high gain d.c. amplifiers used in the simulator is a modest one, it has not been found necessary to resort to automatic drift compensation in them. Manually-operated zeroing controls are provided in the amplifiers and these are adjusted from time to time, as found necessary, between runs.

Solution of Heat Flow Problems

As a final example, a computor is considered in which networks of electrical resistors are used to solve heat flow problems, notably those which arise in the study of the aerodynamic heating of the skin of a missile flying at supersonic speeds. In contrast to the previous examples, the dynamics or kinematics of missile flight are not concerned at all here, and the computor does not employ servo-mechanisms. Its technology is of the simplest kind and it works on no particular time-scale, being manually operated on a step-by-step basis so that the user sets his own pace of making observations. As in the case of the trajectory computor, the main incentive for the building of the machine was the need to reduce the time taken in solving the problems by conventional methods.

Nature of the Problem

For a slab of material bounded by parallel plane faces $x = 0$ and $x = x_n$ and subjected to uniform aerodynamic heating over the plane $x = 0$, the diffusion equation and the boundary conditions are :—

$$\left.\begin{aligned} &\frac{\partial T}{\partial t} = \alpha \frac{\partial^2 T}{\partial x^2} \\ &h\{T_i(t) - T\} = -k \frac{\partial T}{\partial x} \text{ at } x = 0 \\ &\left.\begin{aligned} &T = T_n(t) \\ &\text{or } \frac{\partial T}{\partial x} = 0 \end{aligned}\right\} \text{ at } x = x_n \\ &T = T_0(x) \end{aligned}\right\} \quad (13)$$

In these equations, the symbols have meanings as follows :—

T is the temperature within the material.

$T_i(t)$ is the effective convection temperature, a known function of the time, t.

$T_n(t)$ is the boundary temperature at $x = x_n$ and is a known function of t.

$T_0(x)$ is the temperature within the material at $t = o$ and is a known function of the distance, x.

α is the thermal diffusivity.

k is the thermal conductivity,
and h is the convection coefficient.

These equations are replaced by a set of finite difference equations which are solved by the computor.

If it is written that :—

$$\begin{aligned} x &\equiv r\xi \\ t &\equiv s\tau \\ T(x,t) &\equiv T_{r,s} \\ T_i(t) &\equiv {}_iT_s \\ T_n(t) &\equiv {}_nT_s \\ T_0(x) &\equiv {}_0T_r, \end{aligned}$$

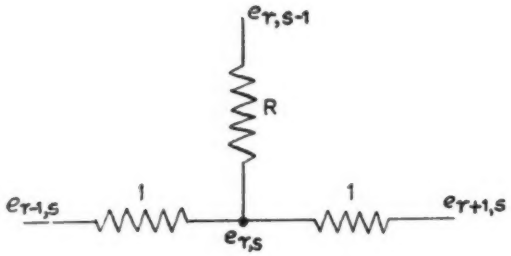

Fig. 7.—Basic network, heat flow computor

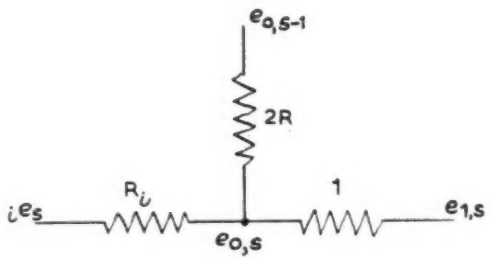

Fig. 8.—Left-hand boundary, heat flow computor

Fig. 9.—Right-hand boundary for $T = T_n(t)$

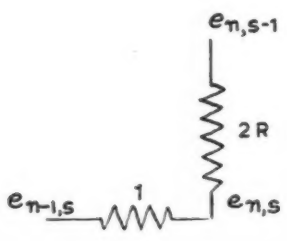

Fig. 10.—Right-hand boundary for $\frac{\partial T}{\partial x} = O$

the finite difference equations become :—

$$\left.\begin{aligned} &T_{r+1,s} - 2T_{r,s} + T_{r-1,s} + \frac{T_{r,s-1} - T_{r,s}}{\alpha\tau/\xi^2} = O \\ &T_{1,s} - T_{0,s} + \frac{T_{0,s-1} - T_{0,s}}{2\alpha\tau/\xi^2} + {}_iT_s - T_{0,s} = O \\ &\left.\begin{aligned} &T_{n,s} = {}_nT_s \\ \text{or } &T_{n-1,s} - T_{n,s} + \frac{T_{n,s-1} - T_{n,s}}{2\alpha\tau/\xi^2} = O \end{aligned}\right\} \\ &T_{r,0} = {}_0T_r \end{aligned}\right\} \quad (14)$$

Formation of the Analogues

Consider the resistance network of Fig. 7. With potentials as shown, the fact that there can be no accumulation of charge at the node (r,s) is expressed by the equation :—

$$e_{r+1,s} - 2e_{r,s} + e_{r-1,s} + \frac{e_{r,s-1} - e_{r,s}}{R} = O \quad .. \quad (15)$$

If this network is iterated, and terminated at the left-hand boundary by the network of Fig. 8, the further equation is :—

$$e_{1,s} - e_{0,s} + \frac{e_{0,s-1} - e_{0,s}}{2R} + \frac{{}_ie_s - e_{0,s}}{R_i} = O \quad .. \quad (16)$$

At the right-hand boundary, two terminations are considered. Corresponding to that of Fig. 9 is the equation :—

$$e_{n,s} = {}_ne_s \quad \ldots\ldots\ldots\ldots\ldots\ldots\ldots\ldots \quad (17)$$

which states that the potential at the node (n,s) is a known function, ${}_ne_s$. Alternatively, for the network of Fig. 10, the equation is :—

$$e_{n-1,s} - e_{n,s} + \frac{e_{n,s-1} - e_{n,s}}{2R} = O \quad \ldots\ldots\ldots \quad (18)$$

Finally for the boundary $s = o$, where the potential is a known function of r,

$$e_{r,0} = {}_0e_r \quad \ldots\ldots\ldots\ldots\ldots\ldots\ldots\ldots \quad (19)$$

Equations (15)-(19) are formally equivalent to the set of equations (14). If $R \equiv \alpha\tau/\xi^2$ and $R_i = \frac{k}{h\xi}$, then the potential at the general node (r,s) will be proportional to $T_{r,s}$.

The Computor

A pilot model of a computor based on the principles previously outlined was first built. In this, the value of s is advanced by unity. If a

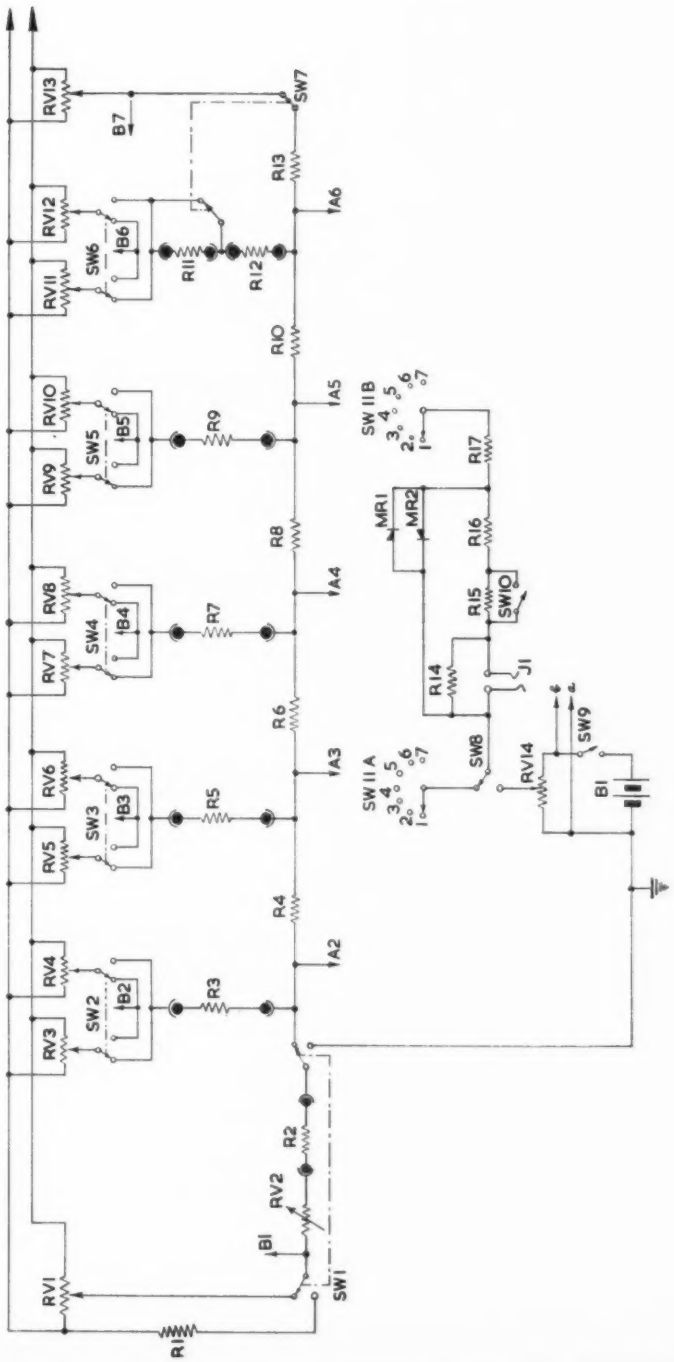

Fig. 11.—Circuit diagram of pilot model of heat flow computor

known temperature distribution $T_{r,s-1}$, and known boundary conditions at the nodes (o,s) and (n,s) are set on the machine, it will compute the temperature distribution $T_{r,s}$. The latter can be fed back into the machine together with the known boundary conditions at the nodes $(o,s+1)$ and $(n,s+1)$ to determine the temperature distribution $T_{r,s+1}$. This process can be continued to any required value of s. There are five nodes in the machine, and the initial temperature distribution ${}_0T_r$ is set on 5 potentiometers (RV3, 5, 7, 9, 11 in the circuit diagram, Fig. 11), the effective convection temperature ${}_iT_1$ being similarly set on a potentiometer RV1. The right-hand boundary condition $T=T_n(t)$ also involves a potentiometer setting, RV13 ; the alternative condition $\frac{\partial T}{\partial x} = O$ is achieved by opening the switch SW7. All potentiometer settings are made by balancing against a standard decade potential divider RV14, using a spot galvanometer plugged into the jack J1 as the null indicator. When the initial values have been set, the potentials at the nodes A2, 3, 4, 5, 6, correspond to the temperature distribution T_{r1}. These values are transferred to a second set of potentiometers RV4, 6, 8, 10, 12, by nulling each of these potentiometers in its turn against the associated node, once again using the galvanometer as the null indicator. By means of the changeover switches, SW2, 3, 4, 5, 6, the original distribution ${}_0T_r$ is replaced by the new distribution T_{r1}. If now the boundary conditions are readjusted to correspond to $s = 2$, the potentials at the nodes will correspond to the distribution T_{r2}. Once again this is transferred, by nulling, to the first set of potentiometers and so the process continues. Potentiometer settings can be determined at any stage of the computation by nulling against the standard divider, whose reading will be a measure of the temperature.

Operating experience with the pilot model indicated that it was an effective computing aid, the solution time of heat flow problems being reduced considerably by its use. It was then decided to build a much larger version, and this machine, which was constructed to the Division's requirements by Messrs. H. W. Sullivan Ltd., has been in service since the beginning of 1955. The principal features of the computor, which is illustrated in Fig. 12, include the following :—

(i) Provision of a greater number of nodes ; the number of stations (including the boundaries) at which the temperature is measured is now 14.

(ii) Allowance for radiative loss at the left hand boundary in addition to convection.

(iii) The use of combinations of coarse and fine controls to increase the accuracy of setting of temperatures and to facilitate operation.

(iv) Simplification and improvement of controls

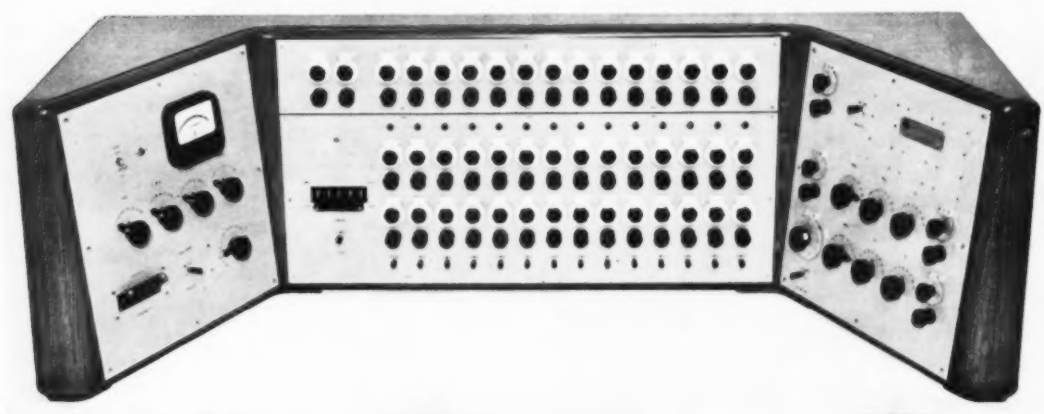

Fig. 12.—Heat flow computor

particularly the transference of temperature distributions.

The basic principles have remained unchanged in the large machine, and the description which has been given of the pilot model remains valid as an introductory account of its successor.

Conclusion

The subject of the present article has by no means been exhaustively illustrated by the three examples of computor which have been described, but it is felt that they constitute a reasonable cross-section of analogue computor design in the guided weapons field, and it is hoped that their description will be of general engineering interest.

Acknowledgements

The author is very much indebted to the staff, past and present, of the Simulator Section of the Guided Weapons Division, who were responsible for the developments described in this paper, and he would especially mention in this connection the names of Mr. H. Marchant and Mr. J. B. Sharp.

RECENT 'ENGLISH ELECTRIC' TECHNICAL PAPERS

I.E.E. Convention on Electrical Equipment of Aircraft, London, May 1956.

WOODALL, R. H., F.R.Ae.S., M.I.E.E. (Rotax Ltd.), DAGLISH, P. J., B.Sc., M.I.E.E., Manager, Aircraft Equipment Division, and HIGGS, V. A., B.Sc., A.M.I.E.E. (British Thomson-Houston Co. Ltd.). *Trends in the development of airborne electrical equipment, with particular reference to constant-frequency alternating-current systems.* Proceedings I.E.E., Paper No. 2089U.

The trend in aircraft design is towards higher altitudes and higher speeds, and the utilization of electrical energy on aircraft is increasing, partly owing to greater aircraft size and partly because of new applications of electrical power, such as de-icing. To meet the increased electrical loads, larger generators will be necessary.

The development of electrical systems and equipment must keep pace with these trends so that equipment is available when new aircraft reach the flight stage. The paper shows the trends in design of electrical systems to meet these conditions.

As altitudes increase, the problem of cooling electrical equipment becomes more difficult, since reductions in air density above 40,000 ft are not accompanied by corresponding reductions in air temperature. The effect on the cooling problem of higher speeds is more serious, since stagnation air temperatures rise with speed, owing to adiabatic compression of the air as the aircraft flies through it, and the rise in temperature in degrees centigrade is proportional to the square of the aircraft speed.

The cooling problem is also accentuated by miniaturization of equipment and by congestion in its installation. It is necessary to consider the electrical system as a whole in order to decide what cooling system should be employed.

The paper shows that, with ram-air cooling, equipment can be designed for satisfactory operation at higher speeds than are possible at the present time, provided that maximum permissible operating temperatures of equipment can be increased.

With d.c. generation, difficult commutation problems are involved when machines are required to operate over a wide range of engine speed. Brush-wear problems under the dry air conditions experienced at high altitudes are well known but far from solved at the present time.

The paper deals with these problems in recommending that, for the future, alternators, preferably brushless and driven at a constant speed, should replace d.c. generators. It is also shown that by this means reliability can be increased and weight per kilowatt generated can be reduced.

The A.C. equipment necessary is discussed, particularly relating to alternators, control gear and motors, and the formidable development problems ahead due to cooling are considered. Emphasis is laid on the necessity for further developments on materials both non-ferrous and insulating to meet future advanced requirements.

Various types of drive are mentioned, and air turbine and hydro-mechanical constant speed drives which have reached an advanced stage of development are discussed in some detail. Their performance characteristics are compared and it is shown that, whereas the hydro-mechanical drive has a considerable advantage on efficiency for certain types of aircraft, there are some installational advantages for the air turbine.

ADCOCK, N. C., A.M.I.E.E., Machine Design Department, and FORD, A. W., B.Sc.(Eng.), A.M.I.E.E., Aircraft Equipment Division. *Excitation systems for A.C. aircraft generators.* Proceedings I.E.E., Paper No. 2133U.

The paper reviews various methods of exciting a.c. aircraft generators, and discusses their relative advantages and limitations in the light of present and future design requirements.

One of the most common methods of exciting a.c. generators is by means of a d.c. exciter built in as an integral part of the generator. It is well known that d.c. exciters are subject to voltage instability at the lower end of the working range,

and sometimes to loss of voltage or to polarity reversal after sudden load changes or fault conditions. Also, in spite of intensive research, the problem of preventing rapid brush wear on commutators and slip-rings at high altitude still awaits a satisfactory solution.

It is suggested that the excitation requirements of present and future high-speed high-altitude aircraft generators will best be met by built-in a.c. exciters designed for 1,600 c/s or 2,400 c/s, supplying the generator field through rectifiers.

With the advent of silicon rectifiers sufficiently small, light and robust to be mounted on a high-speed shaft, it becomes possible to eliminate all sliding contacts from the excitation circuit.

THE
ENGLISH ELECTRIC
COMPANY LIMITED

ALLIED AND ASSOCIATED COMPANIES

English Electric Export and Trading Company Ltd

English Electric Valve Company Ltd

D. Napier & Son Ltd

Marconi's Wireless Telegraph Company Ltd
and its Subsidiaries

The Marconi International Marine Communication Company Ltd
and its Subsidiaries

The Vulcan Foundry Ltd

Robert Stephenson & Hawthorns Ltd

Canadian Marconi Company

John Inglis Co. Limited, Toronto

English Electric Company of Canada Ltd

The English Electric Company of South Africa (Proprietary) Ltd

English Electric de Venezuela, C. A.

The Power and Traction Finance Company Ltd

Associated British Manufacturers (Egypt) Ltd

The English Electric Co. (Central Africa), (Private) Ltd

PRODUCTS OF THE ENGLISH ELECTRIC COMPANY LIMITED

Generating Plant—Steam, Hydraulic, Gas Turbine or Diesel. Transformers, Rectifiers and Switchgear. Industrial Electrification. Electric and Diesel-electric Traction. Marine Propulsion and Auxiliaries. Aircraft. Aircraft Electrical Equipment. Industrial Electronic Equipment. Instruments. Domestic Electrical Appliances.